MONOGRAFIAS DE FÍSICA

XXIII

THE MOSSBAUER EFFECT AND ITS APPLICATIONS

by

D. St. P. Bunbury

University of Manchester

CENTRO BRASILEIRO DE PESQUISAS FÍSICAS

Av. Wenceslau Braz, 71

RIO DE JANEIRO

1965

CONTENTS

-ooOoo-

FOREWORD

The lectures on which these notes are based were given at the "Centro Brasileiro de Pesquisas Físicas" during two months of the winter of 1965.

They were intended for an audience most of whom already had some familiarity with the use of the Mossbauer effect. No attempt was made to provide either a detailed introduction to the field or a comprehensive survey of applications. In fact the choice of subject matter was somewhat arbitrary, some important topics such as relaxation effects in paramagnetics being dismissed rather briefly. The content of the lectures was influenced partly by the current research programme at the "Centro" and partly by the recent interests of the Mossbauer group at Manchester.

I would to thank the staff of the "Centro" for their hospitality during this period and also to acknowledge the assistance of the British Council who made this visit possible by assuming responsibility for the travelling expenses involved.

D. St. P. Bunbury

September 1965

EFFECT ON OBSERVED MOSSBAUER SPECTRUM OF SOURCE AND ABSORBER THICKNESS.

For a thin source the normalized energy distribution of recoilless radiation from an assembly of nuclei in an excited state of mean life $\hbar/2\pi\Gamma$ is

$$W(E)dE = \frac{\Gamma}{2\pi} \frac{dE}{(E-E_0)^2+\frac{\Gamma^2}{4}}$$

Radiation of energy E, in going through an absorber of thickness s, will be attenuated by a factor $\exp\{-ns\sigma(E)\}$ where n is the number of absorbing nuclei of cross section σ per unit volume.

We also have (Heitler, 1949) $\sigma(E) = \frac{\Gamma^2}{4}\sigma_0 \frac{f}{(E-E_0)^2+\frac{\Gamma^2}{4}}$ where σ_0 is the cross section at resonance ($E=E_0$) and f is the recoilless fraction. $\sigma_0 = 2\pi\lambda^2 \frac{2I_e+1}{2I_g+1} \frac{\Gamma_\gamma}{\Gamma}$ where I_e and I_g are the spin of the nucleus in its excited and ground states and Γ_γ is the partial width for decay by radiation. (If internal conversion is the only competing process, then $\Gamma_\gamma/\Gamma = 1/(1+\alpha)$ where α is the internal conversion coefficient).

Suppose that a thin layer dS of the source material gives, in the absence of absorption, an intensity of recoilless radiation at the counter of

$$dI = m f_s ds .$$

Then if the source also contains absorbing nuclei, the energy distribution of the radiation will be altered and the intensity of recoilless radiation will be

$$I(E) = \frac{\Gamma f_s}{2\pi} \int_0^S \frac{m\, ds' \exp\left[-n\sigma_o f_s \Gamma^2 S' \Big/ 4\{(E-E_o)^2 + \Gamma^2/4\}\right]}{\left\{(E-E_o)^2 + \Gamma^2/4\right\}}$$

This is easily integrated:

$$I(E) = 2m \frac{1 - \exp\left[-n\sigma_o f_s S \Gamma^2 \Big/ 4\{(E-E_o)^2 + \Gamma^2/4\}\right]}{\pi n \sigma_o \Gamma} \qquad (2)$$

This reduces to a Lorentzian similar to (1) for small s.

For large s, numerical calculation shows that (2) can be represented quite well by a Lorentzian with an increased width Γ_s. (e.g. Margulies and Ehrman (1961) or Shirley, Kaplan and Axel (1961)).

Writing $t_s = n \sigma_o s f_s$, the intensity at maximum absorption is

$$I(E_o) = \frac{2ms}{\pi \Gamma t_s} f_s \left\{1 - e^{-t_s}\right\} \qquad (3)$$

∴ Total (integrated) intensity of source

$$A = \int_0^\infty I(E)dE = A_o (e^{-t_s/2}) \left\{ J_o\left(\frac{i t_s}{2}\right) - i J_1\left(\frac{i t_s}{2}\right) \right\}$$

where $A_o = m s f_s$ (Integrated intensity in absence of absorption).

Writing

$$\xi = A/A_o \qquad (4)$$

we see that the apparent recoilless fraction becomes $\frac{\xi f_s}{\xi f_s + (1-f_s)}$ which is always less than f_s.

A Lorentzian whose height and area are given by (3) and (4) must have a width Γ_s given by

$$\frac{\Gamma_s}{\Gamma} = \frac{\xi t_s}{1 - e^{-t_s}}$$

This effect is important in Sn^{119}, for example, since the method of source preparation is such that there is always some Sn^{119} in its ground state present. This limits the useable source thickness.

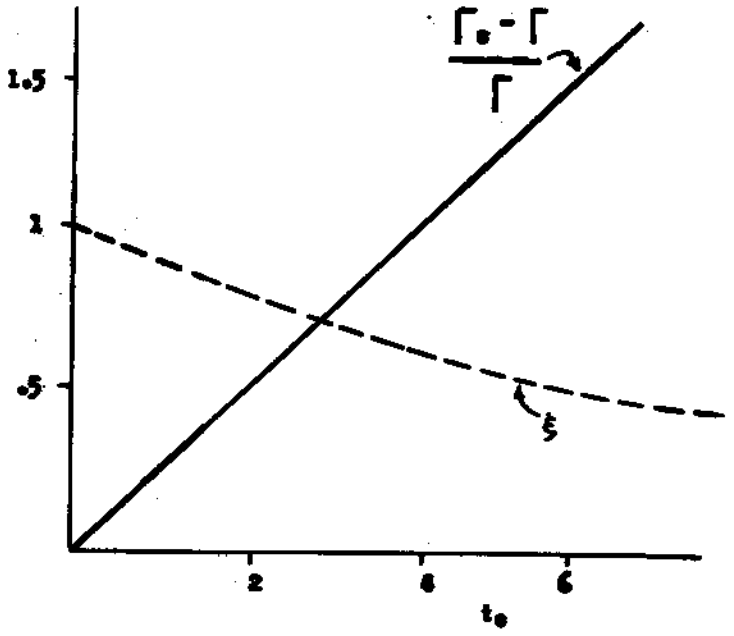

Other causes of broadening such as variations in the environments in which the source nuclei find themselves will generally not affect the area under the emission spectrum. Therefore if we can approximate the actual spactrum a Lorentzian of increased width, the above discussion still holds except that we must use a correspondingly decreased value for σ_o.

We now require to know the intensity transmitted through an absorber of thickness d moving at a velocity v relative to the source.

The number of recoilless γ-quanta is reduced by a factor

$$T(v) = \int_0^\infty W(E) \exp\left\{- n\, d\, \sigma\,(E')\right\} dE \qquad \text{where } E' = E\left(1 + \frac{v}{c}\right)$$

and W(E) is now the actual energy distribution of radiation from

the source (including any broadening) but still normalized to 1.

Since the entire contribution to the integral comes from values of E close to E_o we can extend the integration to $-\infty$, shift the origin to E_o, and replace $E\left(1+\frac{v}{c}\right)$ by $\left(E+\frac{v}{c}E_o\right)$.

$$T(v) = \frac{2\Gamma_s}{\pi}\int_{-\infty}^{\infty}\frac{1}{4E^2+\Gamma_s^2}\exp\left\{\frac{\Gamma_a^2 t_a}{4\left(E+\frac{v}{c}E_o\right)^2+\Gamma_a^2}\right\}dE \quad \ldots \quad (5)$$

where Γ_a is a fictitious width including any broadening of the absorber line, and $t_a = n\,d\,\sigma_o\,f_a$.

This gives the shape of the velocity spectrum but cannot be evaluated explicitly.

A number of special cases are of interest.

If $\Gamma_s = \Gamma_a$

T(v) is given by an infinite series of Bessel functions as shown by Ruby and Hicks (1961).

For $v = 0$, $T_{min} = e^{-t_a/2}\,J_o\left(\frac{it_a}{2}\right)$ exactly.

But so far we have considered only the recoilless part of the radiation from the source so we should introduce a factor βf_s to get the actual decrease in counting rate due to the absorber, where β takes account of the background counting rate (i.e. fraction of counting rate with no absorber which is due to background is $1-\beta$).

Thus $$T_{min} = 1 - \beta f_s\left\{1 - e^{-t_o/2}\,J_o\left(\frac{it_a}{2}\right)\right\}$$

For t_a small (i.e. less than 1) it is a reasonable approxima-

tion to ignore the Bessel function, and for very small t_a, $T_{min} = 1 - \frac{\beta f_s t_a}{2}$. For large values of t_a (up to about 10) the error resulting from putting the Bessel function equal to unity is of the order of 25% or less.

If $\Gamma_s \neq \Gamma_a$ it is more useful to consider the absorption integral,

$$S = N\beta f_s \int_{-\infty}^{\infty} dv \left[1 - \int_{-\infty}^{\infty} W(E) \exp\left\{ - n d \sigma(E') \right\} dE \right]$$

where N is the counting rate at very large values of v.

This can be written (remembering that $\int_{-\infty}^{\infty} W(E)dE = 1$)

$$N \int_{-\infty}^{\infty} dE \left[W(E) \int_{-\infty}^{\infty} \beta f_s \left\{ 1 - \exp\left(\frac{-\Gamma_a^2 t_a}{4\left(E + \frac{v}{c} E_o\right)^2 + \Gamma_a^2} \right) \right\} dv \right]$$

The second integral is independent of E

$$\therefore S = N\beta f_s \int_{-\infty}^{\infty} \left\{ 1 - \exp\left(\frac{-\Gamma_a^2 t_a}{4\left(E + \frac{v}{c} E_o\right)^2 + \Gamma_a^2} \right) \right\} dv .$$

This can be integrated exactly:

$$S = \frac{N f_s \beta \Gamma_a \pi c}{2 E_o} K(t_a) \ldots \qquad (6)$$

where the factor $\frac{c}{E_o}$ converts S to velocity units and

$$K(t) = t\, e^{-t/2} \left\{ J_o\left(\frac{it}{2}\right) - i J_1\left(\frac{it}{2}\right) \right\}$$

Note that we now no longer need to know the form of W(E).

For small t_a

$$S \approx N \Gamma_a \pi n \sigma_o \beta d f_s f_a c/2 E_o$$

So we cannot find f_s and f_a separately using a thin absorber.

However we can find f_a by using absorbers of different thickness and choosing the value of $\sigma_o f_a$ which gives best agreement with expression (6). To eliminate σ_o we must also measure α.

K(t) can be expanded to give

$$K(t) = t(1 - 0.250\ t + 0.0625\ t^2 + \ldots\ldots\ldots\ldots)$$

Returning to expression (5). If the absorber is thin we obtain the approximation

$$T(v) = \beta f_s \left\{ 1 - t_a \frac{\Gamma_a (\Gamma_a + \Gamma_s)}{\frac{4 v^2}{c^2} E_o^2 + (\Gamma_a + \Gamma_s)^2} \right\}$$

Thus the absorption spectrum will have the form of a Lorentzian with a width equal to $(\Gamma_a + \Gamma_s)$.

In the special case $\Gamma_a = \Gamma_s$ numerical integration of (5) shows that, to a good approximation, the absorption spectrum will have the form of a Lorentzian of width;

$$\Gamma = 2 \Gamma_a (1 + 0.135\ t_a) \qquad \text{for } 0 < t_a < 5$$

or

$$\Gamma = 2 \Gamma_a (1 + 0.145\ t_a - 0.0025\ t_a^2) \qquad \text{for } 4 < t_a < 10.$$

Having found f_a we still require to measure Γ_a and βf_s.

This can be done by using the following method due to C. Edwards.

Suppose that we fix a second absorber to the source so that they move together, and let the dimensionless thickness of this absorber be t_2.

Then the recoilless intensity is reduced from $N \beta f_s$ to $N \beta f_s J(t_2, \Delta)$ where

$$J(t,\Delta) = \int_0^\infty W(E) \exp\left\{ \frac{-t_2}{1 + 4 (E - E_o - \Delta)^2 / \Gamma_a^2} \right\} dE$$

where Δ represents a possible energy difference between the resonances of source and absorber (isomer shift).

Then decrease in total counting rate is from N to

$$N \left\{ 1 - \beta f_s + \beta f_s J(t_2, \Delta) \right\}$$

Now use this modified source to measure absorption integral S of another absorber, t_1. Then

$$S'(t_1) = \frac{S(t_1) \; J(t_2, \Delta)}{\left[1 - \beta f_s + \beta f_s J(t_2, \Delta) \right]}$$

Define $\varepsilon(t_2, \Delta) = \beta f_s \left\{ 1 - J(t_2, \Delta) \right\}$.

We can solve these 2 equations for βf_s since we know

$$S(t_1) = \frac{N \beta f_s C \Gamma_a \pi}{2 E_o} K(t_1)$$

$$\therefore \Gamma_a = \frac{S(t_1)}{K(t_1)} \frac{2 E_o}{N \pi c} \frac{\left\{S(t_1) - S'(t_1)\left[1-\varepsilon(t_2, \Delta)\right]\right\}}{S(t_1)\ \varepsilon(t_2, \Delta)}$$

$\varepsilon(t_2, \Delta)$ is just the depth of the absorption spectrum produced by relative motion of source and absorber t_2 and can be measured. Hence we know Γ_a and βf_s. This assumes that the absorber is Lorentzian.

We have throughout neglected atomic absorption. This is usually justified, but in cases where the recoilless fraction is small and the absorber is dilute (i.e. only a small proportion of the atoms in the absorber are of the resonant isotope), non-resonant absorption may be important, not only on account of the reduction in counting rate but, more important, if higher energy radiation makes an important contribution to the background the latter will be increased relative to the resonant radiation. β will then vary with absorber thickness and it will be necessary to estimate the background correction from the pulse-height spectrum of the counter for each absorber used.

A method of determining f_a which avoids this difficulty has been described by Heberle (1964). He used a very thick second absorber as a "shutter" which could be opened by moving it rapidly. Then, since with this arrangement the difference in the counting rates with the shutter open and closed will be due to the recoilless part of the radiation only, a plot of this difference against the velocity of a thin absorber will be a true a absorption curve

for recoilless radiation and will depend on the properties of the absorber only.

A difficulty of the same sort frequently arises in experiments involving the use of the resonant nucleus as the solute in a dilute alloy since the relative background in the counter can be greatly increased as a result of photoelectric absorption in the thick absorbers which are then necessary. In such cases it is usually preferable to use the alloy as the source rather than as the absorber if possible, since if a split source is used with a single-line absorber, only one of the source lines will be absorber at any particular velocity and all the others will be off the resonance. If a single line source is used, the whole emission spectrum will be in resonance with each of the absorption lines in turn.

COMPARISON OF SCATTERING AND ABSORPTION METHODS

Most of the work done so far in the Mossbauer effect has used simple absorption geometry.

This is the most versatile arrangement, but there are other possibilities which may have certain advantages in special cases. We can

a) Count re-radiated photons.

b) Count internal conversion electrons.

c) Count X-rays following internal conversion.

d) Use a combination of one of the above with absorption.

In order to compare the relative merits of those methods it is instructive to make a rough estimate of the statistical accuracy

of a measurement of the Mossbauer effect involving the use of a given source and lasting for a given time.

Suppose that in an absorption experiment we count for long nough to accumulate N counts away from resonance and (1 - A) N a. resonance. Then if we subtract the number of counts at each velocity from N, we get a curve representing the number of photons absorbed.

The height of this peak will be AN and the statistical error on each point $\pm\sqrt{N}$ (if A is small). (Actually this underestimates the error since N is also uncertain).

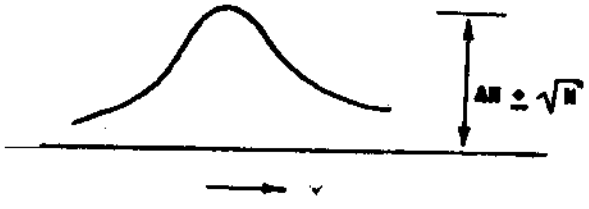

Note that the fraction (1 - A) includes not only non-recoilless radiation from the source and that part of the recoilless radiation which fails to be absorber, but also any background radiation such as γ-rays of other energy, X-rays from the source or from the absorber or even resonantly scattered radiation from the absorber (if the counter is placed too close to it). Some of these contributions to the background can be minimised by care in the design of the apparatus (e.g. use of critical absorbers in suitable cases to remove X-rays, use of a counter with adequate energy resolution etc.).

Now consider the method (a).

The number of resonant scattering events from the same target in the same time will be $AN/(1+\alpha)$ where α is the internal conver

sion coefficient. So if the counter subtends a solid angle Ω at the scatterer the number of counts recorded will be, after correction for background,

$$\frac{\Omega A N}{4\pi(1+\alpha)} \pm \sqrt{\frac{\Omega A N}{4\pi(1+\alpha)} + B} \qquad (7)$$

where B is the number of background counts (i.e. the number of counts obtained at a very high velocity). It is due to direct radiation from the source, Rayleigh scattering and X-rays from the target and its holder etc. Again it can be minimised by careful design. (The error in this case too is an underestimate since it has been assumed that the background counting rate is known exactly.

Comparing the accuracies of the absorption and scattering results we find that the latter have a lower fractional error if

$$4\pi(1+\alpha)\left\{\frac{A}{\Omega} + \frac{4\pi B(1+\alpha)}{N\Omega^2}\right\} < 1 \qquad (8)$$

A small value of B requires good shielding and so makes it difficul to get a large solid angle.

For example, if we take $\Omega/4\pi = .04$ and ignore B, scattering will be preferable to absorption only if $A(1+\alpha) < 1/25$.

One must also take account of practical considerations such as the arrangements for cooling the scatterer (this will almost certainly be necessary in any case in which the recoilless fraction is small enough for scattering to be seriously considered).

These will usually be more difficult in the case of scattering and will tend to make it harder to obtain a large solid angle and low background.

Nevertheless in some cases, particularly of high energy transitions (100 KeV or more), scattering may be the only way in which the Mossbauer effect can be observed. (See, for example Morrison, Atac., De Brunner and Frauenfelder, (1964).

Of course, if a sufficiently strong source is available, the time required to obtain a given statistical accuracy may no longer be the most important consideration in one's choice of method.

The effect of absorber thickness on the shape of the spectrum will be similar to that already considered for absorption in the same scatterer. If the scatterer is thick we must allow for re-absorption of the scattered radiation. We have ignored angular correlations between incident and scattered photons, but this will have to be taken into account in interpreting the relative intensities of the components of complex spectra.

Turning now to the second method, we can make use of internal conversion electrons in two ways. We can either use a very thin absorber in conjunction with a β-ray spectrometer to separate the required line from a strong background, or we can go the opposite extreme of sacrificing energy resolution in favour of obtaining a large solid angle by putting the absorber directly in front of, or even inside the counter.

The first of these methods, owing to its low efficiency

requires a good deal of care to keep down the background counting rate due to direct radiation or to scattering into the counter of electrons ejected from the walls of the spectrometer by higher energy radiation. It has the advantage that it is relatively easy to cool the scatterer. A successful arrangement of this type has been described by Kankeleit (1961).

In the second method, the absorber is deposited on the inside of the window of a counter or incorporated into a plastic scintillator. It is of course important that the counter should have a very low efficiency for direct counting of γ-rays. If a gas-filled counter is used, the maximum absorber thickness will be determined by the range of the electrons produced, but if the absorber is incorporated into a scintillator it can be finely dispersed and the useable thickness will now depend on the transparency of the mixture to light.

Since the factors affecting the efficiency of these methods and the background counting rates will vary so much from case to case it is hardly worth while attempting to make a direct comparison with the absorption method, but we can see that factors favouring the use of internal conversion are, a high conversion coefficient, not too low an energy, and a background which consists mainly of radiation of energy rather close to that of the resonant γ-ray.

Cooling of the absorber is likely to be rather troublesome in this case.

The only entirely successful applications of this method so far have been to Sn^{119} where several groups have found that is more efficient than absorption.

The method suffers from the limitation that it is not easy to change the absorber. However, if a counter of the type described above can be constructed, then since it is selectively sensitive to recoilless radiation, it can with advantage be used to replace the counter in a straightforward absorption experiment. It is, of course, necessary in this case, to keep the source stationary and move the absorber. By reducing the background such a detector can greatly increase the apparent recoilless fraction in an absorption experiment. It has also been shown by Mitrofanov, Illarionova and Shpinel (1963) that the width of the absorption line is decreased, since a resonant detector is most sensitive to the centre of the emission line.

In designing experiments of this type it is necessary to know the range of the internal conversion electrons and the following empirical expression due to Katz and Penfold is useful. The maximum range in mg. cm^{-2} of electrons of energy E MeV in aluminium is given by

$$R = 412\ E^{n}$$

where $$n = 1.265 - 0.095 \ln E$$

Finally we can count X-rays following internal conversion. The efficiency of this method will be similar to that of the scattering method if we replace $\frac{1}{1+\alpha}$ in (7) and (8) by $\frac{\alpha\tau}{1+\alpha}$ where τ is the X-ray

fluorescence yield. However, it may be difficult to obtain a low background since the number of X-rays emitted by the source may greatly exceed the number of resonant γ-rays, and these can undergo Rayleigh scattering in the absorber, and in addition any γ-ray which is absorbed by the photoelectric effect will also cause the emission of an X-ray. X-ray production in the source by β-rays can often be reduced by diluting the source material with some light element such as graphite.

This method has been demonstrated in the case of Fe^{57} by Frauenfelder et al (1961) but does not seem to have been applied to any other cases.

A quite different method which has been used occasionally to reduce the effect of background in an absorption experiment consists of the use of coincidence techniques to select those counting events which are due to the proper transition. Although attractive at first sight this method usually results in a large decrease in counting rate for the following reason. The solid angle Ω_1, subtended at the source by the counter observing the Mossbauer radiation has to be small, as a result of the fact that the Doppler shift of the radiation from a moving source is $E_o \frac{v}{c} \cos\theta$ where $v \cos\theta$ is the component of source velocity in the direction of the path of the photon so that we cannot allow a large range of values of 0. Thus, since the maximum coincidence efficiency will be proportional to $\Omega_1 \Omega_2$ where Ω_2 is the solid angle of the counter observing the coincident transition, we must make $_2$ as large as possible. But the maximum source strength will be that which gives such a counting rate in

one of the counters that excessive loss of energy resolution results, and this will now be determined by counter 2 not counter 1. Thus the maximum genuine coincidence rate will be less by a factor of the order of $\frac{\Omega'}{4\pi}$ as compared to a non-coincidence experiment. In addition, the counting rate may be limited by the need to avoid random coincidences. The number of random coincidences per second will be of the order of $\frac{16\pi^2 G^2 T}{\Omega_1 \Omega_2}$ where G is the genuine coincidence rate and T the coincidence resolving time. For these reasons the coincidence method has not been much used although application [5] have been described by Bonchev et al (1963) and by Hohenemser (1965).

The use of semiconductor counters which combine high energy resolution with a short pulse rise time may make this method more attractive in the future.

PROBLEMS IN THE DESING OF MOSSBAUER SPECTROMETER

The basic apparatus required for the observation of the Mossbauer effect will consist of some means of producing a controlled motion of the source (or absorber), a combination of a counter together with a suitable amplifier and single channel analyzer which one would like to have sufficient energy resolution to give out put pulses only in response to photons originating from the transition being studied, and some means of sorting and storing the counts according to the relative velocity of source and absorber.

We will not consider here the use of constant velocity drives whose main advantage is the relatively simple counting equipment required since the same scalers can be used successively to measure the counting rate at different velocities, nor the various purely

mechanical devices such as screws cams etc. which can be used to produce the required velocity. These have the advantage that they can easily be calibrated by direct measurement, but it is usually simpler to use a known spectrum for calibration.

The most versatile system is undoubtedly the electromechanical transducer or vibrator (loudspeakers are frequently used) which is forced to follow a suitable reference waveform. The waveform most frequently chosen is one which causes the velocity to vary linearly with time (i.e. a triangular velocity waveform). At the usual frequencies of a few cycles per second, this waveform will contain significant harmonics at frequencies above the lowest resonance of the vibrator. In addition, the restoring force of such a vibrator is unlikely to be a strictly linear function of position. It is therefore necessary to use some form of linear velocity to voltage transducer mechanically coupled to the vibrator and to use negative feedback to ensure that the induced voltage accurately follows the reference signal. This transducer will consist either of a coil moving axially in a magnetic field or of a light permanent magnet moving within a fixed coil. A second loudspeaker is often used for the purpose. The condition for linearity is that the ends of the coil should be situated in regions of equal field and this in turn means that either the radial field should be uniform over a region much longer than the coil or it should be confined to a region much shorter than the coil. These conditions are not satisfied by the average loudspeaker whose usefulness is therefore confined to operation at rather small amplitudes.

The accuracy with which the velocity will follow the reference signal depends on the loop gain of the feedback system, and the maximum loop gain which can be employed is determined by the frequency response of the feedback loop. A brief outline will be given here of the principles on which such a system should be designed. For further details one of the standard text books should be consulted (e.g. Thomason. Linear Feedback Analysis).

The figure shows the usual form of schematic diagram for a feedback amplifier.

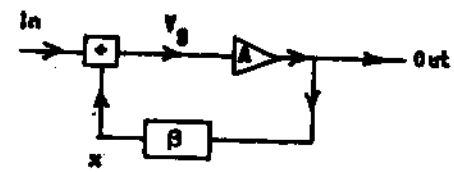

The gain is given by

$$\frac{V_{out}}{V_{in}} = \frac{A}{1 - A\beta} \qquad (9)$$

where $A\beta$ is chosen to be negative at the middle of the pass band. For large values of $A\beta$ this reduces to $-\frac{1}{\beta}$ and this is still true if $A\beta$ is complex and even if its real part becomes positive at certain frequencies. This can be seen from the vector diagram which is drawn for real β and complex A.

The same description applies to a system which is partly electrical and partly mechanical. In the present case, the output is a velocity and β represents the velocity pick-up which is there-

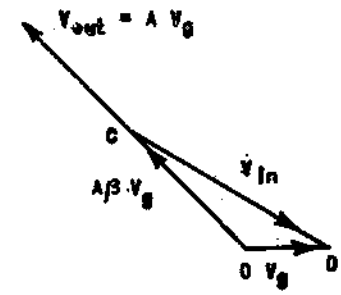

fore the only part of the system which needs to be strictly linear.

If we break the feedback loop at some point such as X, we can measure the open loop gain $A\beta$ as a function of frequency. We define the logarithmic gain relative to some standard frequency ω_o

$$\log \frac{|A(\omega)|}{|A(\omega_o)|} = \alpha(\omega) - \alpha_o$$

This measurement is sufficient to determine completely the behaviour of the loop both when open and when closed (apart from possible frequency dependence of β which we ignore here).

The phase shift introduced by any network is given in terms of the magnitude of the transfer function (i.e. |output/input|) by Bode's theorem:

$$\varphi(\omega) \geqslant \frac{2\omega}{\pi} \int_0^\infty \frac{\alpha(\omega') - \alpha(\omega)}{(\omega')^2 - \omega^2} \, d\omega' \qquad (10)$$

The equality holds for cascaded networks of the simple "ladder" type. The inequality sign only applies to certain cases of more complicated netwoks such as bridges, which are best avoided.

If the loop contains a number of networks of known transfer function connected in such a way, that they do not interact directly, then the total logarithmic gain and phase shift will be simply $\sum \alpha(\omega)$ and $\sum \varphi(\omega)$.

The transfer function of the closed loop may now be written down, but examination of eq. (9) shows that so long as $|A\beta| \gg 1$ both the phase shift and the frequency dependence of gain will be reduced relative to the open loop, but this is no longer true at

frequencies at which $|A\beta| \simeq 1$.

The form of eq. (9) leaves open the question of what happens if the phase shift (relative to the required phase reversal at the mid-band frequency) reaches 180°, so that the feedback is in phase with the input. The answer to this question was given by Nyquist who showed that if we draw the locus of the point C on the vector diagram on the previous page with frequency as a parameter the system will be stable if the curve does not enclose the point D. (For a d.c. coupled feedback loop the closed curve may be completed by reflecting the curve in the real axis, which is equivalent to extending the range of frequency to $-\infty$).

Thus the two diagrams both represent the open loop gains of systems which will remain stable when the loop is closed. The second one is said to be conditionally stable since a reduction of gain by a constant factor will render it unstable. In such an event the amplifier will overload and the analysis which was based on the assumption of linearity will break down. The result is usually that it continues to oscillate even when the amplifier is restored to its original condition. Since such momentary overloading is almost certain to occur at the moment of switching on, conditionally stable feedback

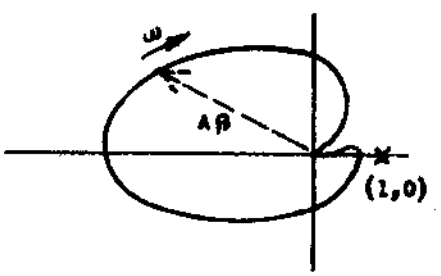

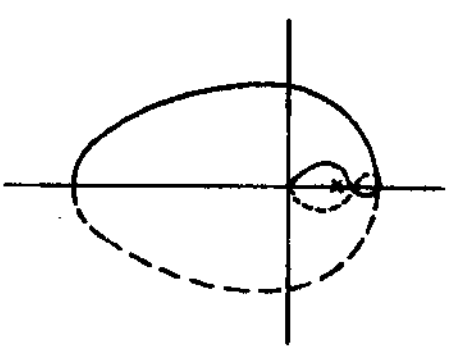

systems are of mainly academic interest and we will not consider them further.

The most general transient response of a linear system (i.e. response to an input of the form $\delta(t)$ is of the form $A_1 e^{P_1 t} + A_2 e^{P_2 t} + \ldots\ldots\ldots$ When Nyquist's condition is not satisfied, at least one of the P's in the solution for the closed loop has a positive real part, and if we change the form of $A\beta$ as a function of ω so that the Nyquist criterion is just satisfied, the real part of P must pass through zero. It is therefore reasonable to suppose that if a feedback system is only just stable, its transient response will contain a term of the form $e^{-\alpha t + j\beta t}$ where α is very small. In other words, it will take a long time to recover from any transient in the input waveform and this recovery will usually have the form of and oscillatory "ringing" at or near the frequency at which the Nyquist diagram comes closest to the critical point. The condition for a satisfactory transient response is thus similar to the condition that the system should be stable with a wide safety margin.

A frequently used rule of thumb is that the Nyquist diagram should lie wholly outside the region shown shaded in the figure. This may be stated approximately as follows. The phase shift of the open loop should not

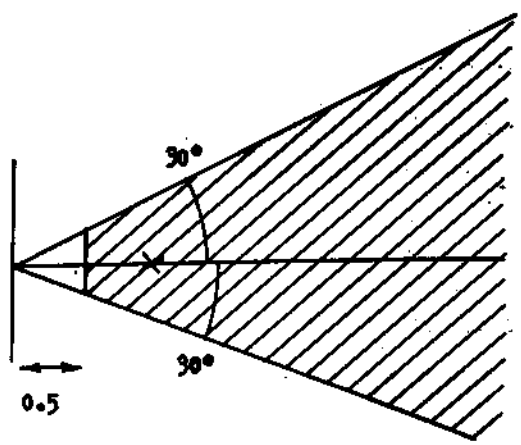

exceed 150° at any frequency at which the magnitude of the loop gain exceeds about 0.6.

From the form of eq. (10) it can be seen that if $|A(\omega)|$ is proportional to ω^n over a reasonable range of frequency, then $\varphi(\omega)$ within that range will be constant and equal to $n\pi/2$. Thus a constant phase lag of 150° corresponds to a drop of the response curve at a rate of about 10 db/octave.

The transfer function of the combination vibrator plus velocity pick-up will have the general form shown somewhat idealized, in the figure.

The slopes below and above the fundamental resonance ω_1, are $\pm$ 90° but at some frequency ω_2 there will be a second resonance due to the compliance of the mechanical coupling between the driving coil and the pick-up coil (or magnet). Above this resonance the phase shift will increase to 270°. In practice it will be difficult to compensate electrically for this resonance and therefore ω_2 represents the frequency by which the loopgain must have fallen to below unity. Clearly it is desirable to make

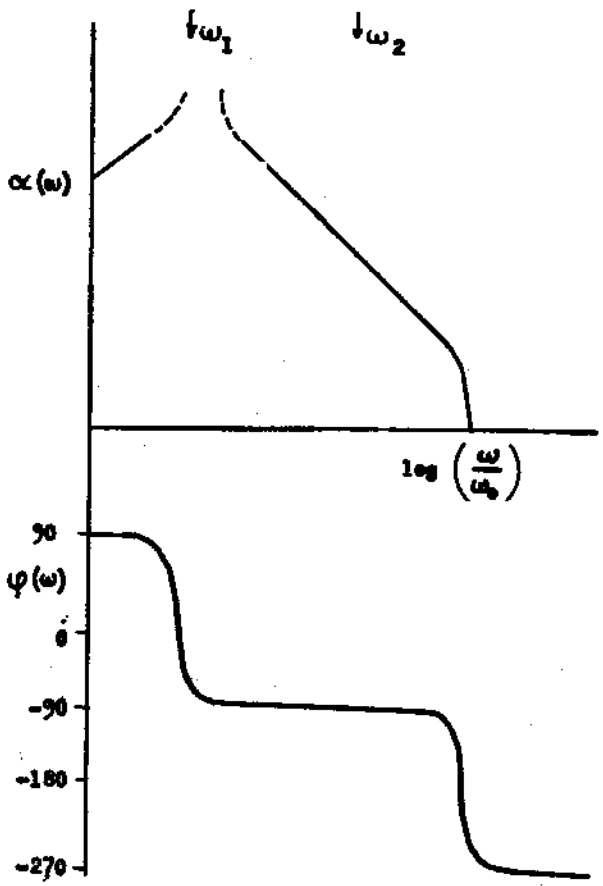

ω_2 as high as possible by using a light but rigid construction for the moving part and placing the drive and pick-up as close together as possible. A frequency of about 6 kc sec^{-1} is not too difficult to achieve. Secondly, in order to obtain a high loop gain at low frequencies the slope of the α v's log ω curve should be as steep as possible having regard to the stability requirements. This means that an additional phase lag of about 60° should be introduced between ω_1 and ω_2. A further phase lag may with advantage be introduced below ω_1, to allow an increase in the low frequency loop gain.

In addition to these resonances there may be resonances associated with standing waves in the diaphragms used for suspension. The effect of these will be to introduce an additional phase lag in the region of the resonance. This may result in instability or conditional stability. To avoid such effects the suspension should be as simple as possible and may be lightly damped by means of plastic foam. A phase advance network can also be used to compensate roughly for the phase shift due to the resonance.

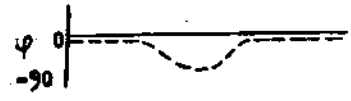

A phase lag of 60° over a wide frequency range is best produced by combining a 90° phase lag

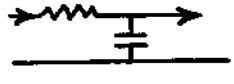

with a series of phase advance networks staggered in frequency in such a way as to produce a more or less constant phase shift of 30^{o}. Final adjustment will usually have to be made by trial and error, the aim being always to obtain a large low frequency loop gain together with a rapidly decaying transient response. Examination of the error signal (V_g in the above diagram) provides a sensitive method of assessing the performance of the system.

A multichannel pulse height analyzer is usually employed for the purpose of sorting and counting pulses from the single channel analyzer (S.C.A.). The methods employed fall into two groups.

We can use the analyzer as a pulse height analyzer by making the signal from the velocity pick-up modulate the output pulses from the S.C.A. or, more directly, by taking the velocity signal straight to the pulse stretcher of the multichannel analyzer and making the S.C.A. signal initiate the sorting operation.

In this method, provided the modulator and analyzer operate linearly, the channel number will be proportional to velocity even if the velocity waveform departs from its ideal shape. However only a triangular velocity waveform will cause equal times to be spent in counting in all channels and therefore any departure from this waveform will result in a distortion of the spectrum. This effect can be avoided by using only half the

available number of channels and counting simultaneously in the other half, pulses corresponding to some non-resonant part of the γ-ray spectrum, using the same modulator. This second spectrum, which should ideally be flat, can be used to correct the Mossbauer spectrum by taking the ratio of counting rates in the corresponding channels of the two halves.

The second method uses the analyzer in the "multiscaler mode" in which counting takes place in a selected channel which can be changed to the next higher one by means of a clock pulse. Thus if there are n channels we can make each channel correspond to a particular velocity if we adjust the clock frequency to exactly n times the vibrator frequency. This can be done by dividing the clock frequency by n, either in an external scaler or by using the address scalar of the analyzer itself and taking the divided signal and a timing signal from the reference waveform generator to a phase comparitor whose output is used to correct the clock frequency. Alternatively the clock frequency can be fixed and a square wave of frequency n times lower used to produce the triangular reference signal (by integration). One again the address scaler can be used as the source of the square wave.

When this method is used, the counting times in all channels will always be equal, but the velocity waveform now determines the horizontal (velocity) scale which will only be linear for a stricly triangular waveform. In this method higher counting rates can be used since in the pulse height analysis mode the dead time of the analyzer is much longer than in the multiscaler mode. (It

is also dependent on channel number in the former mode).

OUTLINE OF THEORY OF THE MOSSBAUER EFFECT

The emission probability of a photon of energy E from a single fixed nucleus is

$$W(E)\,dE = \frac{\Gamma}{2\pi}\,\frac{dE}{(E-E_0)^2+\Gamma^2/4}$$

If the nucleus were free, the photon energy would be reduced by an amount equal to the kinetic energy of the recoiling nucleus $E^2/2\,Mc^2$.

We have to consider the effect of the fact that the nucleus is bound in a crystal lattice and is therefore neither free nor rigidly fixed in space.

The kinetic energy T of a free particle is $p^2/2m$. In the presence of an electromagnetic field A(r), the momentum $\underline{p}$ must be replaced by $\underline{p}\,\frac{eA}{c}$.

Then in the gauge $\nabla\cdot A = 0$, the interaction Hamiltonian is $H' = T - T_0 = -\frac{e}{mc}(\underline{A}\,\underline{p}) + \frac{e}{2mc^2}\underline{A}^2$.

Since we are considering the interaction of a nucleon with the field, the term in A^2, which gives Thompson scattering, is small and will be neglected.

A can be expanded in plane waves of the form

$$\underline{\epsilon}\,\exp(i\omega t - i\,\underline{k}\cdot\underline{r})$$

where $\underline{\epsilon}$ is a unit polarization vector. $e^{i\omega t}$ carries through and can be ignored.

Then if the position $\underline{r}_\alpha$ of the α^{th} nucleon can be written in terms of the position $\underline{R}$ and momentum $\underline{P}$ of the centre of mass and the internal coordinates $\underline{u}_\alpha$ and $\underline{p}_\alpha$ we have for all the nucleons:

$$H' = -\frac{e}{mc}\sum_\alpha e^{i\underline{k}\cdot(\underline{R}+\underline{u}_\alpha)}\,(\underline{P}+\underline{p}_\alpha)\cdot\underline{\epsilon}\,.$$

Since the unperturbed Hamiltonian can be separated into terms involving $\underline{R}$ only and terms involving internal coordinates only, the wave function of the system is a simple product $\Psi(R)\,\varphi(\underline{u}_1, \underline{u}_2 \ldots)$.

Hence the matrix elements of H' will be like this:

$$\langle\Psi_f|H'|\Psi_i\rangle = -\frac{e}{mc}\langle\psi_f|\underline{P}\cdot\underline{\epsilon}\,e^{-i\underline{k}\cdot\underline{R}}|\psi_i\rangle\langle\varphi_f|\sum_\alpha e^{-i\underline{k}\cdot\underline{u}_\alpha}|\varphi_i\rangle$$

$$-\frac{e}{mc}\langle\psi_f|e^{-i\underline{k}\cdot\underline{R}}|\psi_i\rangle\langle\varphi_f|\sum_\alpha e^{-i\underline{k}\cdot\underline{R}}\,\underline{p}_\alpha\cdot\underline{\epsilon}|\varphi_i\rangle \qquad (11)$$

Here $\psi(\underline{R})$ is one of a complete set of lattice states and the $\varphi(\underline{u}_\alpha)$ form a complete nuclear set.

Hence we can use the closure property and each term in the summation over α takes the form:

$$\langle f|H'|i\rangle_\alpha = \frac{-e}{mc}\sum_m\langle\varphi_f|e^{-i\underline{k}\cdot\underline{u}_\alpha}|\varphi_i\rangle\langle\psi_f|e^{-i\underline{k}\cdot\underline{R}}|\psi_m\rangle\langle\psi_m|\underline{P}\cdot\underline{\epsilon}|\psi_i\rangle$$

$$-\frac{e}{mc}\sum_n\langle\varphi_f|e^{-i\underline{k}\cdot\underline{u}_\alpha}|\varphi_n\rangle\langle\varphi_n|\underline{p}_\alpha\cdot\underline{\epsilon}|\varphi_i\rangle\langle\psi_f|e^{-i\underline{k}\cdot\underline{R}}|\psi_i\rangle\,.$$

In this equation, because the momentum of the photon is much greater than the typical lattice momentum we expect that all the matrix elements $\langle\psi_f|e^{-i\underline{k}\cdot\underline{R}}|\psi_n\rangle$ will be of the same order of magnitude as $\langle\psi_f|e^{-i\underline{k}\cdot\underline{R}}|\psi_i\rangle$ and similarly the matrix elements $\langle\varphi_f|e^{-i\underline{k}\cdot\underline{u}_\alpha}|\varphi_n\rangle$ will all be of the same order of magnitude as

$\langle \varphi_f | e^{-i\underline{k}\cdot\underline{u}_\alpha} | \varphi_i \rangle$ since the photon momentum is much smaller than the typical momentum of a nucleon. Hence they can be taken out of the summation and we can write:

$$\langle f|H'|i\rangle = \langle H_1\rangle + \langle H_2\rangle \approx -\frac{e}{mc}\langle \varphi_f | e^{-i\underline{k}\cdot\underline{u}_\alpha} | \varphi_i\rangle \langle \psi_f | e^{-i\underline{k}\cdot\underline{R}} | \psi_i\rangle \sum_m \langle \psi_m | \underline{P}\cdot\underline{\varepsilon} | \psi_i\rangle$$

$$-\frac{e}{mc}\langle \varphi_f | e^{-i\underline{k}\cdot\underline{u}_\alpha} | \varphi_i\rangle \langle \psi_f | e^{-i\underline{k}\cdot\underline{R}} | \psi_i\rangle \sum_n \langle \varphi_n | \underline{p}_\alpha\cdot\underline{\varepsilon} | \varphi_i\rangle$$

$$\therefore \frac{\langle H_1\rangle}{\langle H_2\rangle} \approx \frac{\sum_m \langle \psi_m | \underline{P}\cdot\underline{\varepsilon} | \psi_i\rangle}{\sum_n \langle \varphi_n | \underline{p}_\alpha\cdot\underline{\varepsilon} | \varphi_i\rangle} \approx \frac{\langle P\rangle}{\langle p_\alpha\rangle}$$

i.e. the ratio of the rypical lattice momentum to the typical nucleon momentum. This will be of the order of 10^{-5} and hence we can ignore $\langle H_1\rangle$. We therefore return to eq. (11) dropping the first term. Thus the interaction Hamiltonian can be written as $e^{-i\underline{k}\cdot\underline{R}}$ times the nuclear part where $e^{-i\underline{k}\cdot\underline{R}}$ affects only the centre of mass coordinates of the wave function.

Thus for emission:

$$W(E)dE = \frac{dE\,\Gamma}{2\pi} \sum_{i,f} P_i \frac{|\langle i|e^{-i\underline{k}\cdot\underline{R}}|f\rangle|^2}{(E-E_0+\epsilon_f-\epsilon_i)^2+\Gamma^2/4}$$

where P_i is the relative probability of the initial lattice state i and in the denominator the term representing the change in internal energy of the nucleus is now $(E+\epsilon_f-\epsilon_i)$ instead of E, where $\epsilon_f - \epsilon_i$ is the energy given to the lattice.

We cannot sum over the initial and final states while the lattice energies are in the denominator and we therefore use the following identity.

$$\frac{1}{a^2+b^2} = \frac{1}{2a}\left\{\frac{1}{a+ib} + \frac{1}{a-ib}\right\}$$

$$= \frac{1}{2a}\left\{\frac{1}{\hbar}\int_0^\infty e^{-(a+ib)t/\hbar}\,dt + \frac{1}{\hbar}\int_0^\infty e^{-(a-ib)t/\hbar}\,dt\right\}$$

$$= \frac{1}{2a\hbar}\int_{-\infty}^{+\infty} e^{-ibt/\hbar}\, e^{-a|t|/\hbar}\,dt$$

$$\therefore W(E) = \frac{1}{2\pi\hbar}\sum_{i,f} P_i \langle i|e^{-i\underline{k}\cdot\underline{R}}|f\rangle\langle f|e^{i\underline{k}\cdot\underline{R}}|i\rangle \int_{-\infty}^{+\infty} e^{-i(E-E_o+\epsilon_f-\epsilon_i)t/\hbar}$$

$$e^{-\Gamma|t|/2\hbar}\,dt$$

This is independent of the origin of time. We replace t by $t - t_o$. We also use the fact that if $\mathcal{H}$ is the crystal Hamiltonian, then

$$e^{i\mathcal{H}t/\hbar}|n\rangle = e^{i\epsilon_n t/\hbar}|n\rangle$$

$$\therefore W(E) = \frac{1}{2\pi\hbar}\sum_{i,f} P_i \int_{-\infty}^{+\infty} e^{-\Gamma|t|/2\hbar}\, e^{-i(E-E_o)t/\hbar}\langle i|e^{\frac{i\mathcal{H}t_o}{\hbar}}\, e^{-i\underline{k}\cdot\underline{R}}\, e^{-\frac{i\mathcal{H}t_o}{\hbar}}|f\rangle$$

$$\times\langle f|e^{\frac{i\mathcal{H}t}{\hbar}}\, e^{i\underline{k}\cdot\underline{R}}\, e^{-\frac{i\mathcal{H}t}{\hbar}}|i\rangle$$

The operators in the matrix elements in this equation define the Heisenberg position operators $\underline{r}(t)$.

.. If the equation is written in terms of r(0) and r(t), the crystal energies no longer appear in the denominator and since the final states form a complete set we can sum by closure:

$$W(E) = \frac{1}{2\pi\hbar}\int_{-\infty}^{+\infty} dt\, e^{-\frac{\Gamma|t|}{2\hbar}}\, e^{\frac{i(E-E_o)t}{\hbar}} \left\langle e^{-i\underline{k}\cdot\underline{r}(0)}\, e^{i\underline{k}\cdot\underline{r}(t)}\right\rangle_T \qquad (12)$$

where $\left\langle e^{-ik\underline{r}(0)}\, ik\underline{r}(t)\right\rangle_T$ denotes the average expectation value of the enclosed operator at temperature T,

$$\text{i.e. } \sum_i P_i \langle i|.....|i\rangle$$

This expression is quite general. The Mossbauer effect arises as a result of the properties of the expectation value. Note that if the latter is independent of time then the above expression is just the Fourier integral corresponding to a Lorentzian of width Γ centred on $E = E_o$.

Let us define functions $F_s(\underline{k}, t)$ and $G_s(\underline{r}, t)$ such that

$$\left\langle e^{-i\underline{k}\cdot\underline{r}(0)}\, e^{i\underline{k}\cdot\underline{r}(t)}\right\rangle_T = F_s(\underline{k}, t) = \int d\underline{r}\, e^{i\underline{k}\cdot\underline{r}}\, G_s(\underline{r}, t) \qquad (13)$$

i.e. $G_s(\underline{r}, t)$ is the Fourier transform of $F_s(\underline{k}, t)$.

$$\therefore W(E) = \frac{1}{2\pi\hbar}\int_{-\infty}^{+\infty} dt \int d\underline{r}\, \exp i\left\{\underline{k}\cdot\underline{r} + (E-E_o)\frac{t}{\hbar}\right\} e^{-\frac{\Gamma|t|}{2\hbar}}\, G_s(\underline{r}_1 t) \qquad (14)$$

If we interpret $\underline{r}$ as a classical coordinate, we can attach a simple physical meaning to $G_s(\underline{r}, t)$, the self-correlation function.

We can write:

$$G_s(\underline{r},t) = \frac{1}{(2\pi)^3}\int d\underline{k}\, e^{-i\underline{k}\cdot\underline{r}} \left\langle e^{-i\underline{k}\cdot\underline{r}(0)}\, e^{i\underline{k}\cdot\underline{r}(t)}\right\rangle_T$$

$$= \frac{1}{(2\pi)^3} \int d\underline{k} \int d\underline{r}' \, e^{-i\underline{k}\cdot\underline{r}} \langle e^{i\underline{k}\cdot\underline{r}(0)} \, e^{i\underline{k}\cdot\underline{r}'} \, \delta(\underline{r}'-\underline{r}(t)) \rangle_T$$

$$= \frac{1}{(2\pi)^3} \int d\underline{r}' \int d\underline{k} \, \langle e^{-i\underline{k}\cdot\underline{r}} \, e^{i\underline{k}\cdot\underline{r}(0)} \, e^{i\underline{k}\cdot\underline{r}'} \delta(\underline{r}' - \underline{r}(t)) \rangle_T$$

$$= \int d\underline{r}' \, \langle \delta(\underline{r} + \underline{r}(0) - \underline{r}') \, \delta(\underline{r}' - \underline{r}(t)) \rangle_T$$

$G_s(\underline{r},t)$ gives the probability that a nucleus which was at $\underline{r}(0)$ at time 0 will be at $\underline{r}(0) + \underline{r}$ at time t.

We see that if the nucleus is fixed, $\underline{r}(t) = \underline{r}(0)$ and $G_s(\underline{r},t) = \delta(\underline{r} - \underline{r}(0))$, so that

$$W(E) = \frac{\Gamma}{2\pi} \frac{1}{(E-E_o)^2 + \Gamma^2/4}$$ as expected.

In general, if $G_s(\underline{r}, t)$ becomes independent of time after a certain time, then the integrals over $\underline{r}$ and t become independent and the shape of W(E) will be a Lorentzian of width Γ but reduced in amplitude by a factor which will be small unless the time required for $G_s(\underline{r},t)$ to become constant is much less than the nuclear lifetime $\hbar/\Gamma$ and it is then confined to a region of dimensions small compared to the wavelength 1/k.

This gives the recoilless part of the emission spectrum.

$G_s(\underline{r}, t)$ will become independent of time as the correlation between $\underline{r}(0)$ and $\underline{r}(t)$ disappears.

The figure shows, qualitatively the behaviour of $G_s(\underline{r},t)$ and $F_s(\underline{k},t)$. $G_s(\underline{r},t)$ is a δ-function at t = 0 but broadens with time

due to lattice vibrations until, after a few vibration periods, it becomes independent of time and represents simply the probability distribution of the atom about its mean position.

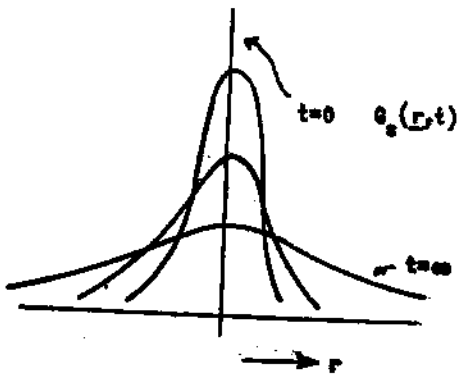

At the same time $F_s(\underline{k},t)$ decays from unity at t=0 to a constant value. This value can be taken outside the integral in eq. (12) and is just the recoilless fraction.

The time dependent part will result in a broadened (and in general also shifted) energy spectrum as can easily be seen by supposing the time dependence to be exponential and substituting in eq. (12). (It will, of course, actually be much more complicated).

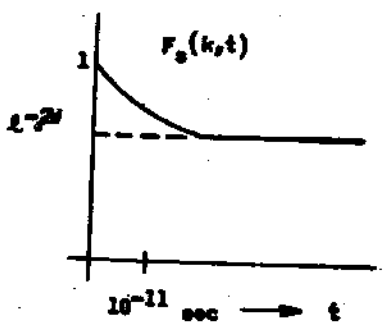

At times large compared to the period of the lattice vibrations we can write

$$F_s(\underline{k},t) = \int d\underline{r}\, e^{i\underline{k}\cdot\underline{r}} \int d\underline{r}' \langle \delta(\underline{r}+\underline{r}(0)-\underline{r}') \rangle_T \langle \delta(\underline{r}'-\underline{r}(\infty)) \rangle_T$$

since the arguments of the δ functions will no longer be correlated at large times.

$$\therefore F_s(\underline{k},t) = \int dr' \left\langle e^{i\underline{k}\cdot\underline{r}' - i\underline{k}\cdot\underline{r}(0)} \right\rangle_T \left\langle \delta(\underline{r}' - \underline{r}(\infty)) \right\rangle_T$$

$$= \left\langle e^{-i\underline{k}\cdot\underline{r}(0)} \right\rangle_T \left\langle e^{i\underline{k}\cdot\underline{r}(\infty)} \right\rangle_T$$

$$= \left\{ \left\langle e^{i\underline{k}\cdot\underline{r}} \right\rangle \right\}^2$$

which is therefore the recoilless fraction, often written e^{-2W}.

Strictly, $G_s(\underline{r}, t)$ and $F_s(\underline{k},t)$ never become completely independent of time since after the initical broadening of $G_s(\underline{r},t)$ due to the lattice vibrations it will continue to spread at a much slower rate as a result of diffusion. This will be specially marked in the case of a liquid. The consequences of diffusion will be considered later.

What we have said so far applies, strictly, only to emission. Scattering and absorption are more complicated since we cannot, in principle, say which nucleus in the crystal is responsible. We should therefore consider interference between the different nuclei. (In the first chapter we assumed that the absorbing nuclei could be regarded as acting completely independently and we shall see that this approximation is usually justified in practice).

It can be shown that the cross section for scattering into a solid angle $d\Omega$ is

$$\frac{d^2\sigma}{d\Omega dE'} = \frac{\gamma}{2\pi} \frac{\mu\Gamma^2}{4} \sum_{i,f} P_i \left| \sum_m \sum_M \frac{\langle i|e^{i\underline{k}\cdot\underline{r}_m}|M\rangle \langle M|e^{i\underline{k}'\cdot\underline{r}_m}|f\rangle}{\left\{(E'-E-\epsilon_f-\epsilon_i) - \frac{1}{2}i\gamma\right\}\left\{(E'-E_o+\epsilon_f-\epsilon_M) - \frac{1}{2}i\Gamma\right\}} \right|^2$$

where E is the energy of the centre of the incident line, E' is the

energy of the scattered photon, $\underline{k}$ and $\underline{k}'$ are the corresponding wave vectors, γ and Γ are the widths of the incident radiation and of the scattering level, $\mu = \frac{\Gamma_\gamma}{\Gamma} \frac{\sigma_o}{4\pi} f(\theta,\varphi)$ where $f(\theta,\varphi)$ describes the angular dependence of the nuclear matrix elements and is normalized to 4π, and the sums over m and M are over all the relevant nuclei and over all the states of the lattice respectively.

Starting from this expression we proceed by methods exactly analogous to those used in the case of emission. The main steps in the calculation are outlined in the review article by Boyle and Hall (1962). Here we will only quote the results.

If we write $\underline{r}_m(t) = \underline{R}_m + \underline{u}_m(t)$ where $\underline{R}_m$ is the mean position of the m^{th} nucleus, we obtain

$$\frac{d^2\sigma}{d\Omega dE'} = \mathrm{Re}\ \mathrm{Pt}\left[\frac{\mu\Gamma}{2\pi\hbar^2}\sum_{m,n}\int_{-\infty}^{\infty}d\tau\int_{0}^{\infty}d\tau_1\ \exp.\left\{\frac{-\frac{1}{2}\gamma|\tau|-\frac{1}{2}\Gamma\tau_1+i(\underline{E}_o-\underline{E})\tau+i(\underline{E}'-\underline{E}_o)(\tau+\tau_1)}{\hbar}\right\}\right.$$

$$\left.\times\left\langle e^{i\underline{k}\cdot\underline{u}_m(0)}e^{-i\underline{k}\cdot\underline{u}_n(\tau)}\right\rangle_T\left\langle e^{-i\underline{k}'\cdot\underline{u}_m(0)}e^{i\underline{k}'\cdot\underline{u}_n(\tau+\tau_1)}\right\rangle_T\right.$$

$$\left.\exp\left\{i(\underline{k}-\underline{k}')(\underline{R}_m-\underline{R}_n)\right\}\right] \qquad (15)$$

where we have already made use of the assumption that the correlation between the position operators $\underline{u}_m$ and $\underline{u}_n$ disappears in a time much shorter than $\hbar/\Gamma$.

As before, that part of the expectation values which is independent of time will give rise to recoilless scattering.

We will consider a few special cases.

If we take the time independent parts of both expectation values in (15) we obtain the recoilless part of the scattering (i.e. the scattering which we would observe using a resonant detector):

$$\frac{d^2\sigma}{d\Omega dE'} = \frac{\gamma}{2\pi}\,\frac{\mu\Gamma}{4}\,e^{-4W}\,\frac{\sum_{m,n} e^{i(\underline{k}-\underline{k}')\cdot(R_m - R_n)}}{\left\{(E'-E)^2+\frac{1}{4}\gamma^2\right\}\left\{(E'-E_o)^2+\frac{1}{4}\Gamma^2\right\}} \tag{16}$$

The summation in the numerator over all pairs of resonant nuclei is the familiar Bragg factor which is sharphy peaked in certain directions. It is interesting to notice that if the energy of the incident radiation is displaced from resonance by a few times $(\gamma+\Gamma)$ the energy distribution of the scattered radiation has two peaks, one centred on E, and one on E_o. These will be of the same intensity if $\gamma = \Gamma$.

The total recoilless scattering at a given angle is obtained by integrating over E':

$$\frac{d\sigma}{d\Omega} = \frac{\mu\Gamma(\gamma+\Gamma)}{4}\,e^{-4W}\sum_{m,n}\,\frac{e^{i(\underline{k}-\underline{k}')\cdot(\underline{R}_m-\underline{R}_n)}}{(E-E_o)^2+\frac{1}{4}(\gamma+\Gamma)^2} \tag{17}$$

To obtain the total resonant scattering we must include the case where only the first expectation value in (15) is time independent. This is the scattering which one would observe using a non-resonant detector:

$$\frac{d\sigma}{d\Omega} = \frac{\mu\Gamma(\gamma+\Gamma)}{4} e^{-2W} \sum_{m,n} \frac{\langle e^{-i\underline{k}'\cdot\underline{u}_m(0)} e^{i\underline{k}'\cdot\underline{u}_n(0)}\rangle e^{i(\underline{k}-\underline{k}')\cdot(\underline{R}_m-\underline{R}_n)}}{(E-E_o)^2+\frac{1}{4}(\gamma+\Gamma)^2} \qquad (18)$$

This expression reduces to (17) if the vibrations of all atoms in the crystal are uncorrelated, but in general there will be an additional term due to the short-range correlations of $u_m(0)$ and $u_n(0)$. The peaks in the angular distribution will be broadened by an amount depending on the range of this correlation. This corresponds to the "thermal diffuse" component of X-ray scattering.

The radiation in the peak centred on E in eq. (16) will be coherent with the incident radiation as will be the radiation scattered by atomic electrons (Rayleigh scattering). We might therefore expect to see interference effects between these two forms of scattering. A formal analysis shows that this is indeed the case. The effect of this interference can be recognized due to the fact that the phase of the resonant term changes by π as one goes through the resonance. The two forms of scattering interfere constructively for $E > E_o$, destructively for $E < E_o$. The effect is further complicated by the different polarizations and structure factors of the two forms of scattering.

The above calculations neglected the effect of internal conversion and of the fact that the resonant isotope may not be the only one present, in which case only a certain proportion of the sites will contribute to the lattice sum in the case of resonant scatter

ing. For these reasons, it is usually safe in simple absorption experiments to treat the absorbing nuclei as if they acted independently, particularly if the absorber is polycrystalline. The absorption process is then just the inverse of emission.

However, in suitably designed experiments it is quite possible to observe interference effects of the types outlined above and the theoretical results have been confirmed experimentally by Black et al (1964), who have also given a more detailed account of the theory.

Another interesting consequence of the interference between resonant scattering by different nuclei is the possibility of observing total reflection from the surface of the scatterer. This effect has been studied by Bernstein and Campbell (1963) (See also Bernstein and Newton 1965).

We will not consider interference effects any further here. We will regard absorption as simply the reverse of the emission process and we will now return to eq. (12) in order to consider how the recoilless fraction is related to the properties of the crystal lattice.

$$W(E) = \frac{1}{2\pi\hbar}\int_{-\infty}^{\infty} d\tau\, e^{-\frac{\Gamma|\tau|}{2\hbar}}\, e^{i(E-E_0)\tau/\hbar}\, \langle e^{-i\underline{k}\cdot\underline{r}(0)}\, e^{i\underline{k}\cdot\underline{r}(\tau)}\rangle \quad \ldots (12)$$

It can be shown that this can be written in the form

$$\frac{1}{2\pi\hbar}\, e^{-2W}\int_{-\infty}^{\infty} d\tau\, e^{-\frac{\Gamma|\tau|}{2\hbar}}\, e^{i(E-E_0)\,\tau/\hbar}\, e^{\langle \underline{k}\cdot\underline{r}(0)\;\; \underline{k}\cdot\underline{r}(\tau)\rangle}$$

(Maradudin (1964)), where $2W = \langle(\underline{k}\ \underline{r})^2\rangle = k^2 \langle x^2\rangle$ provided the lattice forces are harmonic. Here x is the component of the mean square vibrational amplitude in the direction of emission. By expanding $r(\tau)$ in terms of normal coordinates of the crystal, substituting in $e^{\langle \underline{k}\cdot\underline{r}(0)\ \underline{k}\cdot\underline{r}(\tau)\rangle}$ and picking out the terms which are time-independent it can be shown that $e^{\langle \underline{k}\cdot\underline{r}(0)\ \underline{k}\cdot\underline{r}(\tau)\rangle}$ reduces to unity in the limit where the number of normal modes involved is very large.

To calculate $2W$, we can either start with $\langle x^2\rangle$ and proceed as follows, or else use Van Hove's expression for $G(\underline{r}, t)$ for a solid.

A simple Bravais lattice will have 3 N oscillators of frequency ω_j, each of average energy $(\bar{n}_j + \frac{1}{2})\hbar\omega_j$ where $\bar{n}_j$ is given by:

$$\bar{n}_j = \frac{1}{\exp\left(\frac{\hbar\omega_j}{k_B T}\right) - 1}$$

$\therefore$ That part of the energy of the crystal which is attributable to the j^{th} oscillator is:

$$NM\omega_j^2 \langle r_j^2\rangle = (\bar{n}_j + \tfrac{1}{2})\ \hbar\ \omega_j$$

where r_j is the contribution to the displacement of the atoms due to the j^{th} oscillator.

Summation over j gives

$$\langle r^2\rangle = \frac{\hbar}{NM} \sum_j \frac{(\bar{n}_j + \frac{1}{2})}{\omega_j}$$

Then if we introduce a density of vibrational states $\rho(\omega)$ and replace the $\sum$ by an integral, we have , putting $\langle x^2 \rangle = \frac{1}{3} \langle r^2 \rangle$

$$\langle x^2 \rangle = \frac{\hbar}{3NM} \int_0^{\omega_{max}} \left\{ \frac{1}{2} + \frac{1}{\exp\left(\frac{\hbar\omega}{k_B T}\right) - 1} \right\} \frac{\rho(\omega)}{\omega} \, d\omega \,. \qquad (19)$$

This allows us to calculate the Debye-Waller factor, e^{-2W}, in terms of the vibrational spectrum of the lattice.

Alternatively, we can start from eq. (14) and use Van Hove's expression for the general form of $G_s(\underline{r}, t)$ for a solid. (Van Hove, 1954). Also Glauber, 1955).

$$G_s(r, t) = \left\{ 2\pi g(t) \right\}^{-3/2} \exp\left\{ -r^2 \Big/ 2g(t) \right\} \qquad (20)$$

where for an isotropic monatomic cubic lattice,

$$g(t) = \frac{\hbar^2}{M} \int_0^{\infty} \left\{ \left(1 - \cos \frac{2t}{\hbar} \right) \coth\left(\frac{2}{k_B T} \right) - i \sin \frac{2t}{\hbar} \right\} \frac{f(z)}{z} \, dz$$

where $f(z)$ is the normalized density of phonon states.

Substituting (20) into (14) and integrating over $\underline{r}$ one obtains

$$W(E) = \frac{1}{2\pi\hbar} \int_{-\infty}^{\infty} dt \; e^{i(E-E_0)\frac{t}{\hbar} - \frac{\Gamma|t|}{2\hbar}} \; e^{-\frac{1}{2}k^2 g(t)}$$

We have seen that the recoilless part of the emission is given by that part of the correlation function which is independent of time and this will be given by $g(\infty)$.

So we obtain for the recoilless part:

$$W_o(E) = \frac{e^{-\frac{1}{2}k^2 g(\infty)}}{2\pi\hbar} \int_{-\infty}^{\infty} dt\, e^{i(E-E_o)\frac{t}{\hbar} - \frac{\Gamma|t|}{2\hbar}}$$

$$\therefore 2W = \tfrac{1}{2} k^2 g(\infty) = \frac{\hbar^2 k^2}{2M} \int_0^{\infty} \coth \frac{z}{2 k_B T} \frac{f(z)}{z} dz$$

This is easily shown to agree with eq. (19) if it is remembered that

$$\int_0^{\infty} \rho(\omega) d\omega = 3N$$

In order to proceed any furhter we must use some model to give $\rho(\omega)$.

In the Debye model, $\rho(\omega) = \dfrac{q N \omega^2}{\omega_{max}^3}$

$$\therefore 2W = \frac{3\hbar k^2}{M} \int_0^{\omega_{max}} \left\{ \frac{1}{2} + \frac{1}{\exp\left(\frac{\hbar\omega}{k_B T}\right) - 1} \right\} \frac{\omega}{\omega_{max}^3} d\omega$$

or, writing $\omega_{max} = k_B \theta_D/\hbar$,

$$2W = \frac{3\hbar^2 k^2}{M k_B \theta_D} \left\{ \frac{1}{4} + \left(\frac{T}{\theta_D}\right)^2 \int_0^{\theta_D/T} \frac{x}{e^x - 1} dx \right\} \qquad (21)$$

θ_D, the Debye temperature is usually known from specific heat measurements.

Tables are available for the evaluation of (21). (A. H. Muir. Atomics International div. of N. American Aviation. Report No AI 6699).

In the limit of low temperature $\left(\frac{\theta_D}{T} \gtrsim 5\right)$

$$\int_0^{\theta_D/T} \frac{x\,dx}{e^x - 1} \approx \frac{\pi^2}{6}$$

while in the high temperature limit (i.e. $T \gtrsim \theta_D$)

$$2W \approx \frac{6E_R}{k_B} \frac{T}{\theta_D^2}$$

where E_R is the kinetic energy of a freely recoiling atom; $h^2k^2/2M$.

All this applies strictly only to a monatomic lattice.

The presence of optical modes will usually increase the recoilless fraction for a given Debye θ, since they make an important contribution to the specific heat but, as a result of their high frequency, they have rather little effect on the recoilless fraction.

It has been shown by a number of authors that if the resonant nucleus occurs as an impurity, its effective θ will be the same as if all atoms in the crystal had the mass of the impurity but the binding forces were those characteristic of the binding of the impurity in the actual crystal. (Vischer (1963); Maradudin (1964); Disatnik, Fainstein and Lipkin (1965)).

In cases where the Debye approximation is not a good one, it may still be convenient to represent the behaviour in terms of a single parameter θ_n even though it may be necessary to allow it to vary with temperature. It might be possible to calculate the

phonon spectrum from the known structure of the crystal if we knew the exact from of the interaction between the atoms. This of course is not the case but we may be able to estimate a value of the cut-off frequency (corresponding to θ_M) from the density of points in reciprocal space and the positions of the Brillouin zones of the crystal. In this method we assume that the velocity of long wavelength phonons (which are the important ones from our point of view) can be calculated from macroscopically measured elastic constants. In this way it is possible to derive an expression for θ_M in terms of the elastic constants.

A crystal in which the forces were accurately harmonic would show no thermal expansion. It is therefore necessary to allow θ_M to vary with temperature on account of the change in frequency of the normal modes which results from a change in volume.

Only in a few cases has any attempt been made to compare measured and calculated values of the Debye-Waller factor over a wide temperature range, metallic Fe and Sn being probably the two examples for which the most complete data are available.

For Fe the results agree with calculations from the Debye model over a wide temperature range, but begin to deviate at temperatures of several hundred degrees. It seems that the experiments need to be extended to still higher temperatures (Baijal (1964)).

The case of Sn illustrates the care which is necessary in

measurements of this kind. The early work of Boyle, Bunbury, Edwards and Hall (1961) on Sn^{119} showed deviations from the Debye model which were explained in terms of anharmonicity of the lattice forces. This interpretation was found to be hard to reconcile with the conclusions of Feldman and Horton (1963) and of De Wames and Lehman (1964) who determined the dispersion curves for the Sn vibrational spectrum using the measured elastic constants. As the Mossbauer measurements had been of the peak absorption as a function of temperature and thus depended on the assumption of constant width for the absorption line, they were repeated using the area under the absorption curve as a measure of the Debye-Waller factor. It was then found that the width is, in fact, markedly temperature dependent and the new results, after correction for thermal expansion, are in reasonable agreement with those obtained by the elastic constant method. The reason for the variation in width of the absorption line is not understood and is still being investigated.

As has been pointed out, the Debye approximation cannot be expected to describe the behaviour of alloys and compounds, and only qualitative comparisons between theory and experiment have been possible. However, as has been pointed out by Gol'danskii (1964), a comparison between the temperature variations of the recoilless fractions of a Mossbauer nucleus in different environments can yield useful information about the chemical binding. An extreme example has been described by the Jerusalem group (Hazony and Hillman, (1965)) who found that the recoilless frac-

tion of Kr^{83} in a clathrate dropped initially with increasing temperature but them become almost constant above about 140°K. This behaviour is suggestive of a model in which the gas atom is trapped in a steep sided potential well, and is consistent with the usual picture of a clathrate, although the recoilless fraction seems to change much more rapidly with temperature below 140°K than one would expect.

In a crystal of symmetry lower than cubic, the recoilless fraction may well be anisotropic. This has been observed in a number of cases and has some important consequences which will be described later.

.It may also be mentioned that the temperature dependence of the relativistic energy shift (second order Doppler effect) can also give information about the phonon spectrum of a solid. The interpretation is complicated by the fact that a temperature-dependent isomer shift may also be present. However, it can sometimes usefully be employed to supplement measurements of Debye-Waller factor.

APPLICATION OF THE MOSSBAUER EFFECT TO THE STUDY OF DIFFUSION

It was mentioned earlier that it is not atrictly correct to regard the function $G_s(\underline{r},t)$ as becoming time-independent at large values of t, since the atom under consideration will continue to drift away from its initial position by a process of diffusion. It is of some interest to consider whether the Mossbauer effect can be used to observe this diffusion and this section will be devoted to a discussion of some work recently carried out at Manchester on this question.

Examination of the expression for F in terms of G Eq.(13) shows that if $G_s(\underline{r},t)$ widens with increasing t, then the fall-off of F will be characterised by a time of the order of that taken for $G_s(\underline{r},t)$ to spread to a width $1/k$. Hence for a nuclear lifetime t_o, we can expect to observe a broadening of the line if the diffusion coefficient is of the order of $1/k^2\ t_o$. For Fe^{57} this implies a very viscous liquid.

Diffusion is generally through of as proceeding by two mechanisms. First there is the continuous diffusion process characteristic of gases for which it is easily shown that the probability distribution of a particle about its initial position is a Gaussian function whose mean square width is proportional to time.

$$\text{i.e.}\quad G_s^{CD}(\underline{r},t) = \frac{1}{\left\{2\pi a^2(t)\right\}^{3/2}} \exp\left\{-\frac{r^2}{2a^2(t)}\right\} \qquad (22)$$

where the mean square distance $a^2(t) = 2D_c t$, D_c being the ordinary diffusion coefficient.

The second mechanism requires the diffusing particle to move in discrete jumps between fixed lattice points. This is the mechanism of diffusion in solids. We can present a much simplified picture of this type of diffusion by supposing that an atom can jump to any one of n surrounding sites and that it has a probability $1/\tau$ per unit time of making a jump. Then if $P(\underline{r})$ is the probability that the atom is at $\underline{r}$, we have;

$$\frac{\partial P(r)}{\partial t} = \frac{1}{n\tau} \sum_{\underline{e}} \left\{P(\underline{r}+\underline{\ell}) - P(\underline{r})\right\}$$

where the summation is over the n available sites surrounding $\underline{r}$.

Then $G_s(\underline{r},t)$ is just the solution of this equation with the boundary condition $G_s(\underline{r},0) = \delta(\underline{r})$.

If we use a trial solution of the form

$$G_s^{JD}(\underline{r},t) = (2\pi)^{-3} \int e^{-i\underline{k}\cdot\underline{r}}\, e^{-\ell(k)t}\, d\underline{k} \qquad (23)$$

we find that

$$\ell(k) = \frac{1}{n\tau} \sum_{\underline{l}} (1 - e^{-i\underline{k}\cdot\underline{l}})$$

If we now make the further approximation of assuming that all the available sites lie on a sphere of radius R (the mean interatomic distance) we find,

$$\ell(k) = \frac{1}{\tau}\left(1 - \frac{\sin kR}{kR}\right) \qquad (24)$$

The diffusion coefficient can be shown to be $D_j = R^2/6\tau$.

Diffusion in a liquid can be through of as involving a combination of both these mechanisms; molecules jump between sites which are themselves in the process of continuous diffusion.

There are two ways in which we can study diffusion in a liquid. The first is to use the Mossbauer effect as an analyzer to study the broadening of a γ-ray line which has undergone non-resonant coherent scattering in the liquid, and the second is to perform a simple absorption experiment in which either the source or the absorber is incorporated into the liquid. We will consider the latter method first.

The liquid used was supercooled glycerol which was chosen because it has a relatively simple molecule and has suitable values

of diffusion coefficient over a convenient temperature range. Enriched $Fe_2^{57}(SO_4)_3$ was dissolved in the glycerol. It was subsequently found that some of the Fe^{+++} had been accidentally reduced to Fe^{++} but this proved to be no disadvantage since the different quadrupole splittings (zero for Fe^{+++}) and isomer shifts allowed the two contributions to the spectrum to be separated quite easily.

The relative absorption A(s) at a velocity $\frac{Sc}{E_o}$ for a thin absorber is

$$A(S) \alpha \int_{-\infty}^{\infty} W(E-S)\, \sigma_a(E) dE$$

where, as before

$$W(E) = \frac{\Gamma_s}{2\pi} \ell_s \int_{-\infty}^{\infty} dt\, e^{i\omega t}\, e^{-\frac{\Gamma_s |t|}{2\hbar}}$$

$$\sigma_a(E) = \frac{\Gamma_a^2}{4} \int_{-\infty}^{\infty} dt\, e^{i\omega t}\, e^{-\frac{\Gamma_a |t|}{2\hbar}}\, F_s(\underline{k},t)$$

$\therefore$ If the Fourier transform of A(s) is A(t), then

$$\bar{A}(t) \alpha\, e^{-\frac{(\Gamma_a+\Gamma_s)|t|}{2\hbar}}\, F_s(\underline{k},t)$$

Remembering that $F_s(\underline{k},t) = \langle e^{-i\underline{k}\cdot\underline{r}(0)}\, e^{i\underline{k}\cdot\underline{r}(t)} \rangle_T$, we express the position $\underline{r}(t)$ of a nucleus as the sum of two terms

$$\underline{r}(t) = \underline{r}^V(t) + \underline{r}^D(t)$$

which are respectively the vibrational part of the displacement and the diffusive part, and we assume that these are uncorrelated

$$\therefore F_s(\underline{k},t) = F_s^V(\underline{k},t)\, F_s^D(\underline{k},t) = e^{-2W}\, F_s^D(\underline{k},t)$$

after a few vibration periods. So,

$$\bar{A}(t) \propto e^{-\frac{(\Gamma_a+\Gamma_s)|t|}{2\hbar}}\, F_s^D(\underline{k}, t)$$

If we further assume that continuous and jump diffusion are uncorrelated, we can write $F_s^D = F_s^{CD}\, F_s^{JD}$. Then since $G_s(\underline{r},t)$ is the Fourier transform of $F_s(\underline{k},t)$, eq's (22), (23) and (24) give us

$$F_s^D(\underline{k},t) = e^{-\frac{t}{\tau}\left(1 - \frac{\sin kR}{kR}\right)} e^{-\frac{1}{2}a^2(t)k^2} \qquad (26)$$

Thus both types of diffusion lead to a broadened line which is still Lorentzian, but the dependence on k is different.

If we take the Fourier transform of the experimental absorption line and divide it by $e^{-\frac{(\Gamma_a+\Gamma_s)|t|}{2\hbar}}$ (i.e. by the Fourier transform of the unbroadened line, assumed to be that obtained experimentally with the absorber at a low temperature) we are left with $F_s^D(\underline{k}, t)$ times an unknown constant, and a plot of the logarithm of this quantity against t should be a straight line of slope

$$-\frac{1}{\tau}\left(1 - \frac{\sin kR}{kR}\right) - \frac{1}{2}\frac{a^2(t)}{t}\, k^2$$

If we put $R = 4 \times 10^{-8}$ cm for glycerol and $k = 7.3 \times 10^8$ cm^{-1} (equivalent to 14.4 keV), then we find that even when we take the smallest possible value of τ (i.e. $\tau = R^2/6D$ where D is the measured macroscopic diffusion coefficient) the first term in this expression is two orders of magnitude less than the experimental va-

lue of this slope. We therefore assume that the broadening of the absorption line is entirely due to continuous diffusion.

$$\text{i.e.} \quad \ln F_s^D(\underline{k},t) = -\frac{k^2}{2}\,\frac{a^2(t)}{t} + \text{const.}$$

The figure shows the form of the results for an absorber at 0°C. It will be seen that after an initial rapid rise, both curves show a discontinuity of slope at about 10^{-8} sec and thereafter become roughly parallel. Presumably the slope at large values of t corresponds to the macroscopically observed diffusion. The corresponding diffusion coefficient, given by $D_c = a^2(t)/2t$ is about a factor four times less than the measured value, which suggests that at this temperature jumps make a contribution to the diffusion coefficient about three times greater than that due to the continuous process. (Bunbury Elliott Hall and Williams (1963)).

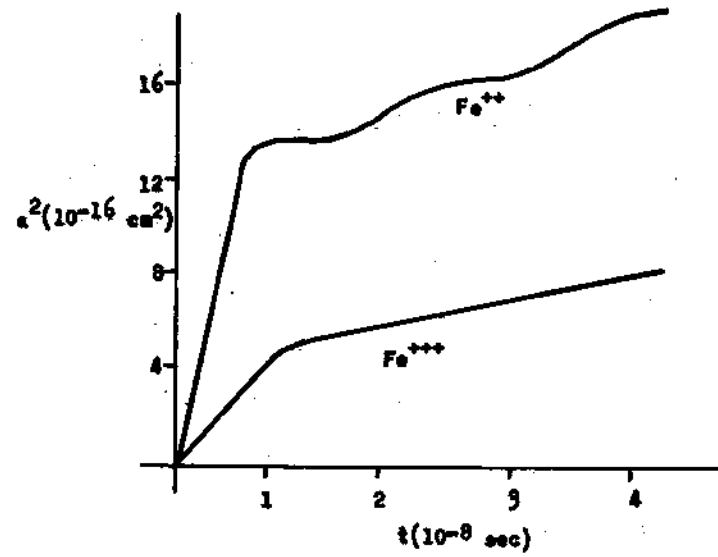

Two suggestions have been put forward to account for the initial rapid rise in a^2. (Note that the time scale, 10^{-8} sec., is several orders of magnitude longer than that of the decay of correlations in the vibrational motion).

The Fe ion is probably carried by a glycerol molecule, and

the initial spreading of $G_s(r,t)$ could be due to rotation of the molecule. Nuclear magnetic resonance measurements on the protons in glycerol at this temperature suggest that the time scale is about right.

The second explanation, due to Singwi and Robinson (1964) postulates that the Fe ion is trapped in a shell of surrounding glycerol molecules and that the broadening of the Mossbauer line is due to a combination of diffusive motions of the ion within the shell and of the shell itself.

Again, rough quantitative calculations give agreement with the experimental results.

The results at $0^{\circ}C$ were chosen for detailed analysis because this temperature represented the best compromise between the conflicting requirements of a large broadening (high temperature) and a large value of e^{-2W} (low temperature). Results obtained at other temperatures were in general agreement with those at $0^{\circ}C$ but with larger statistical errors. The maximum thickness of the absorber was limited by photoelectric absorption and the consequent increase in relative background counting rate. It is possible that the measurements could be extended to higher temperatures if the liquid were used as the source instead of as the absorber. It might also be advantageous to use covalent ionorganic liquids rather than Hydrogen bonded liquids such as glycerol.

It should, in principle be possible to observe diffusive broadening of the Mossbauer line in a solid at a temperature suf-

ficiently close to the melting point. However, we have seen that rather a large diffusion coefficient is required to give a detectable broadening in the case of jump diffusion. A reported observation of diffusion in Sn near the melting point (Boyle Bunbury Edwards and Hall (1961)) has now been shown to be in error (Longworth and Packwood, (1965)), the observed effect being due to premelting in the impure sample used.

The other method of observing diffusive broadening, using the Mossbauer effect to analyse non-resonantly scattered radiation, should in principle give rather more information since the momentum transfer now depends on the scattering angle and hence can be varied at will. However the experimental difficulties are considerable and extremely strong sources are needed to give results with sufficiently low statistical errors for useful conclusions to be drawn from them.

It will be remembered that the interaction Hamiltonian between a charged particle and the electromagnetic field was,

$$H' = -\frac{e}{mc}(\underline{A}\cdot\underline{p}) + \frac{e}{2m\,c^2}\underline{A}^2$$

Previously the charged particle under consideration was a nucleon and we were able to neglect the second term, but as we are now considering scattering by electrons (Rayleigh scattering) the second term will be the dominant one.

If we now proceed in the same manner as before with this exception, we arrive at the following expression for the scatter-

ing cross section:

$$\frac{d^2\sigma_s}{d\Omega dE} = \frac{\alpha^2}{Nh\Gamma} \int_{-\infty}^{\infty} dt\, e^{\frac{i(E-E_o)t}{h}} e^{-\frac{\Gamma|t|}{2h}} \sum_{m,n} \langle e^{-i\underline{k}\cdot\underline{r}_m(0)} e^{i\underline{k}\,\underline{r}_m(t)} \rangle_T$$

where α^2 is a constant, Γ is the width of the incident Lorentzian line centred on E_o, E is the energy of the scattered radiation and $\underline{K}$ is the momentum transfer; $\underline{K} = \underline{k} - \underline{k}_o$ where the magnitudes of $\underline{k}$ and $\underline{k}_o$ are the same. N is the number of scattering centres and the summation is over all pairs.

We define $F(\underline{k},t) = \frac{1}{N} \sum_{m\ n} \langle e^{-i\underline{k}\cdot\underline{r}_m(0)}\ e^{i\underline{k}\cdot\underline{r}_m(t)} \rangle$

(which reduces to $F_s(\underline{k},t)$ if m = n).

As before, we can write $\underline{r}$ as a sum of terms

$$\underline{r}_m(t) = \underline{R}_m + \underline{u}_m^V(t) + \underline{u}_m^{CD}(t) + \underline{u}_m^{JD}(t)$$

where the terms are respectively the mean initial position, the vibrational displacement and the displacements due to continuous and jump diffusion.

Then in the approximation in which these terms are uncorrelated, we can write $F(\underline{K},t)$ (after a few vibration periods when the correlations between $u^V(0)$ and $u^V(t)$ will have disappeared) as;

$$F(K,t) = \left\{ \frac{1}{N} \sum_{m\ n} \langle e^{i\underline{K}\cdot(R_n - R_m)} \rangle \right\} e^{-2W} \langle e^{-i\underline{K}\cdot\underline{u}^{CD}(t)} \rangle_T \langle e^{-i\underline{K}\cdot u^{JD}(t)} \rangle_T$$

since we can put $\underline{u}^{CD}(0) = \underline{u}^{JD}(0) = 0$ and take $u^{CD}(t)$ and $u^{JD}(t)$ outside the summation.

The first factor is the Bragg factor F(K,0) and the last

factors are F_s^{CD} and F_s^{JD}

$$F(K,t) = F(K,0)\, e^{-2W}\, F_s^{CD}(K,t)\, F_s^{JD}(K,t)$$

Thus the diffusive broadening of the scattered line also depends on the self-correlation function.

The angular dependence of the Bragg factor for a liquid takes the form of a broad ring at an angle of the order of λ/R.

For 14.4 keV radiation scattered off glycerol, the maximum occurs at about 12^o and has a width of about 5^o. This effectively determines the range of angles which it is possible to use with a source of given intensity.

Measurements were made as a function of angle at a temperature of -12^oC which again represents a compromise between broadening and intensity of coherent scattering. The results were analyzed as before and can be summarized as follows.

The results could only be followed out to times of about 10^{-8} sec with reasonable accuracy. Plots were made of $-\ln F_s^D(K,t)$ against k^2 for constant values of t. Then eq. (26) shows that these should be straight lines at large values of k^2 which should allow one to find the continuous diffusion coefficient from their slopes and the jump diffusion coefficient by extrapolating the linear portion back to $k = 0$. The results confirm that both continuous and jump diffusion must be taken into account, although the actual values obtained, $D^J \approx 2 \times 10^{-8}$ cm^2 sec^{-1} and $D^C \approx 6 \times 10^{-9}$ cm^2 sec^{-1} are rather larger than the value of dif-

fusion coefficient calculated from the viscosity. In view of the anomalous results observed in the absorption experiments at times less than 10^{-8} sec this is perhaps not too surprizing.

The source strength used in this experiment was 100 mC. The useful solid angle was limited by the need for adequate angular resolution to define K. The statistical accuracy was limited by the background of incoherently (non-recoillessly) scattered radiation which increased with increasing temperature. It has been estimated that in order to analyse the shapes of the scattered lines in as much detail as was done in the case of the absorption experiments it would be necessary to increase the source strength by at least another factor of ten, although the situation might be eased considerably if a really satisfactory resonant counter for 14,4 keV could be made.

Finally it is of interest to compare the type of information given by these experiments with that obtained by neutron scattering. The wavelengths used in the two methods are of the same order of magnitude (about 10^{-8} cm) but the energy resolution of neutron time-of-flight methods is about 10^{-4} eV which corresponds to a time of about 10^{-12} sec., while the corresponding figures for the Mossbauer effect in Fe^{57} are about 10^{-8} eV and 10^{-8} sec. Thus neutron scattering is suitable for the observation of much higher rates of diffusion and has, in fact, been applied sucessfully to the study of liquid metals. Thus there is a large gap between the ranges accessible to the two methods and it would

seem to be desirable to make observations using wider as well as narrower Mossbauer lines. However, as has been pointed out, the practical difficulties are considerable even with Fe^{57}. In passing we may note two other differences between the neutron and Mossbauer methods. Firstly, the neutron method applied to glycerol detects the motion of individual protons rather than of the molecule as a whole, and secondly as a result of the short time of observation it is probably not correct to ignore correlation between diffusive and vibrational motion and the correlation function involved is not $G_s(\underline{r},t)$ but $G(\underline{r},t)$ which does not contain any restriction as to the identity of the particles whose positions are observed at times 0 and t.

A rather fuller account of the theory of diffusive broadening of a Mossbauer line will be found in the paper by Singwi and Sjolander (1960).

THE ISOMER SHIFT

In the interaction of a nucleus with the static electric and magnetic fields due to its surrounding, only three terms are of importance. These are the monopole interaction with the charge density at the position of the nucleus, the interaction between the nuclear magnetic dipole moment and the magnetic field in which it is situated, and the interaction between the electric quadrupole moment of the nucleus and the applied electric field gradient. In this section we consider the first of these, which gives rise to the effect known as the isomer shift (by analogy with the isotope

shift in optical spectrocopy).

If we suppose that the nucleus is replaced by an equivalent spherical charge distribution of radius R then the difference of electrostatic potential due to the nucleus from that which would result from a point nucleus of the same charge is

$$\begin{cases} \Delta V(r) = Ze \int_r^R \left(1 - \frac{r^3}{R^3}\right)\frac{dr}{r^2} = -Ze\left(\frac{3}{2R} - \frac{1}{r} - \frac{r^2}{2R^3}\right), & \text{for } r < R \\ \Delta V(r) = 0, \quad \text{for } r > R \end{cases}$$

Then that part of the total energy of the atom which is due to the finite extension of the nucleus is

$$\delta E = \int \rho \Delta V(r) dV$$

where $\rho = -e|\psi(0)|^2$, the charge density at the position of the nucleus due to the surrounding electrons.

$$\therefore \delta E = 4\pi Ze^2 \int_0^R r^2 |\psi(0)|^2 \left(\frac{3}{2R} - \frac{1}{r} - \frac{r^2}{2R^3}\right) dr =$$

$$= \frac{2\pi Ze^2 R^2}{5} |\psi(0)|^2$$

If we have two states of the nucleus with different R

$$\delta E_{ex} - \delta E_g = \frac{2\pi}{5} Ze^2 |\psi(0)|^2 \left(R_{ex}^2 - R_g^2\right)$$

This can, of course, not be measured, but we can measure the change in this difference when we change $|\psi(0)|^2$.

Thus,

$$S = \frac{2\pi}{5} Ze^2 \left\{|\psi_1(0)|^2 - |\psi_2(0)|^2\right\}\left\{R_{ex}^2 - R_g^2\right\} =$$

$$= \frac{4\pi}{5} Ze^2R^2\left(\frac{\delta R}{R}\right)\left\{|\psi_1(0)|^2 - |\psi_2(0)|^2\right\} .$$

So we can make relative measurements by using a particular substance as a standard (e.g. as absorber), and then observing relative shifts in other absorber using the same source.

This simple classical treatment ignores certain relativistic corrections and also the distortion of the wave function by the field of the nucleus.

The problem has been considered by Bodmer (1961) who found that

$$S = \frac{4\pi R_H}{Z} \frac{a_H^3}{2\left\{\Gamma(2\rho)\right\}^2} \frac{\alpha Z - \frac{2}{5}(1+\rho)\ Z(1+0.106\alpha^2Z^2+\ldots)}{\alpha Z - \frac{2}{5}(1-\rho)\ Z(1+0.106\alpha^2Z^2+\ldots)}\left(\frac{2Z}{a_H}\right)^{2\rho} \tag{27}$$

$$\times \left\{|\psi_1(0)|^2 - |\psi_2(0)|^2\right\} R^{2\rho}\left(\frac{\delta R}{R}\right)$$

where R_H is the Rydberg constant, a_H is the Bohr radius of Hydrogen, α is the fine structure constant, $\rho = (1-Z^2\alpha^2)^{\frac{1}{2}}$ and $\psi(0)$ is the non-relativistic wave function at the origin. R is now the radius of the equivalent uniform charge distribution. (The shift actually depends on the $(2\rho)^{th}$ moment of the nuclear charge).

Thus we can write, in terms of velocity units:

$$\delta v = \frac{v_o}{E_o} F(Z) \frac{\delta R}{R} \left\{|\psi_1(0)^2| - |\psi_2(0)|^2\right\}$$

Shirley (1964) has given a table which can be used in calculat

ing F(Z).

In the non-relativistic approximation, only s electrons contribute to the charge density at the nucleus, but a relativistic calculation shows that in high-Z atoms, there can be an appreciable contribution from $p_{\frac{1}{2}}$ electrons also.

The s electron density at the nucleus will be affected by mutual shielding of the electrons. Thus the outer s electrons can shield inner closed s shells from the nucleus and ns electrons can themselves be shielded by other ns electrons and also by valence electrons in other sub shells. Thus if the occupancy of one of the subshells changes it is necessary to consider the effect on the charge density at the nucleus, of the change in the screening of all the other s electrons.

The usual methods for evaluating $|\psi_s(0)|^2$ make use of the Fermi Segrè formula Goudsmit (1933):

$$|\psi_{ns}(0)|^2 = \frac{Z\, Z_{eff}^2}{\pi\, a_H^3\, n_o^3} \left(1 - \frac{d\sigma}{dn}\right)$$

where Z_{eff} is the effective charge felt by the electron (usually taken, before correction for screening, as 1 + m where m is the charge on the atom or ion), n_o is the effective quantum number = $= n - \sigma$ where σ is the quantum defect. All these parameters can be found by optical spectroscopy.

In some cases information about the value of $\psi_{ns}(0)$ can be obtained by other means. For example, the hyperfine splitting

of an electronic s level can be observed spectroscopically and depends on the overlap of the magnetic dipole moment distributions of the electron and of the nucleus. This leads to the expression:

$$|\psi_{ns}(0)|^2 = 2.54 \times 10^{26} \left\{ a_{ns}/K(Z)\ g_I \right\} \quad cm^{-3}$$

where a_{ns} is the experimental hyperfine splitting in cm^{-1}, K(Z) is a correction factor which varies from 1 for low Z to 2 for high Z and g_I is the nuclear moment in nuclear magnetons. (Kopferman (1958).

Crawford and Shawlow (1949) have shown how to calculate the screening constants. The essentials of their method will be described with reference to the example of Sn^{119}.

An increase in the number of electrons in the 5s shell will have the effect of reducing the field felt by the other s shells since part of their wave functions lie outside part of the wave function of the 5s electron, and hence the effective charge for the ns electrons will be reduced by an amount p given by

$$p = \int_0^{\infty} \varphi_{ns}^2(r_1) \int_0^{r_1} \varphi_{5s}^2(r)\ dr\ dr_1$$

where φ_{ns}^2 is the radial density distribution of the ns electron. The value of p can be calculated using Hartree wave functions. Then, since σ is a slowly varying quantity, the Fermi-Segré formula will give:

$$\frac{\Delta|\psi_{ns}(0)|^2}{|\psi_{ns}(0)|^2} = \frac{\Delta Z^2_{eff}}{Z^2_{eff}} = \frac{Z^2_{eff} - (Z_{eff} - p)^2}{Z^2_{eff}} = \frac{2p}{Z_{eff}}$$

where Z_{eff} is the apropriate value for the ns shell. Hartree wave functions are then used to give $\frac{|\psi_{ns}(0)|^2}{|\psi_{5s}(0)|^2}$, so that we now have the change in ns electron density in units of $|\psi_{5s}(0)|^2$.

If the number of 5p electrons is different in the two absorbers being compared, it will be necessary to calculate the screening by 5p electrons in the same way. The mutual shielding of the 5s electrons is taken into account by assuming that, since half the wave function of each lies inside that of the other, each contributes 1/2 to the effective charge seen by the other. The apropriate value of n_o is calculated from the ionization potentials.

In the original calculation of $\frac{\delta R}{R}$ by Boyle Bunbury and Edwards (1962) it was assumed that the most ionic stannic and stannous compounds (Sn F_4 and Sn Cl_2) are completely ionic and so have the configurations $4d^{10}$ and $4d^{10}5s^2$. The calculation is rather simple in this case since the two differ by just two 5s electrons. The total screening correction summed over all electrons is then equivalent to 0.23 of a 5s electron. So the total electron density difference at the nucleus should be $1.54|\psi_{5s}(0)|^2_{F.S}$ where $|\psi_{5s}(0)|^2_{F.S}$ is given by the Fermi Segrè formula as 1.6×10^{26} cm^{-3}. Eq. (27) then gives $\frac{\delta R}{R} = (1.2 \pm .14) \times 10^{-4}$ when the experimental isomer shift of 5.2 mm $sec.^{-1}$ is inserted. This figure is almost certainly too small since Sn F_4 and Sn Cl_2 are not fully ionic. There is some disagreement about the correct form of the relation between

electronegativity and bond ionicity. Shirley (1964) bases his estimate of $\frac{\delta R}{R}$ upon the isomer shift between Sn F_4 and α-Sn($5s5p^3$) assuming Sn F_4 to be 85% ionic. The result obtained was 1.16×10^{-4} but again this is likely to be too small since no allowance was made for shielding by the 5p electrons in α-Sn. However, Gold'danskii has recently come to the conclusion that the ionicity of Sn F_4 is not more than 40%. This means that all the Sn Halides must be corrected for shielding by 5p electrons. Taking this into account, Bersuker Gold'danskii and Makarov (1965). Also Gold'anskii and Makarov (1965) have recalculated the s-electron densities for the alkali halides. They find that, contrary to expectation, the density at the nucleus increases as one proceeds in the direction of increasing bond ionicity. This requires that $\frac{\delta R}{R}$ must be negative; in other words the radius of the nuclear charge distribution is greater in the ground state than in the excited state. These calculations have not yet been extended to compounds other than the stannic halides and tetrahedral Sn (grey Sn) and Gol'danskii et al have only been able to place a limit on $\frac{\delta R}{R}$; $\frac{\delta R}{R} < -1.6 \times \times 10^{-4}$. Clearly the situation is still rather unsatisfactory. It is possible that a measurement of the shift of the Sn^{119} line as a function of pressure might be the best way of obtaining an unambiguous answer.

In spite of the uncertainty in the absolute calibration of the scale of s-electron density versus isomer shift, much useful information can be derived from measurements of relative shifts in different compounds. Measurements have been made in a large

number of Sn compounds including many organic compounds. The interpretation of these results will not be considered here. They have been discussed by Gol'danskii (1963 and 1964).

An attempt to predict the value of $\frac{\delta R}{R}$ on the unified model as modified by Kisslinger and Sorensen to take account of pairing forces between the nucleons has been described by Boyle Bunbury and Edwards (1962). For this purpose it was assumed that the observed change in effective charge radius is due to a change in deformation without change of volume. The predicted value is about 1.0×10^{-4}. It seems that it would be rather difficult to explain a negative value.

The isomer shift of Fe^{57} has been even more extensively studied. The free atom has the configuration $3d^6\ 4s^2$ and the divalent and trivalent ions are usually taken to be $3d^6$ and $3d^5$, which differ only by a 3d electron. Gol'danskii (1964) quotes some evidence based on the fine structure of X-ray absorption edges that the actual configurations are different from these quoted. However the arguments used are rather indirect and there is a good deal of evidence to support the usual interpretation). It is again assumed that the most ionic compounds are completely ionic. The isomer shift is then due to the change in screening of the filled 3s shell by the 3d electron. The calculation proceeds as described above and leads to a value of $\frac{\delta R}{R}$ for Fe^{57} of -1.8×10^{-3}. (Walker Wertheim and Jaccarino (1961)).

Isomer shift measurements have been made on a number of other

elements, but only in the cases of Eu, I and Au have they been at all systematic.

Iodine is interesting because it is one of the very few non-metals which can be used in Mossbauer studies. Hafemeister De Pasquali and De Waard (1964) measured the isomer shift in all the alkali iodides and also in several iodates and periodates.

NMR chemical shift data give the number of holes in the p shell. This varies from ~0 for KI to ~. 15 for LiF and CsI . The isomer shift follows this data closely, indicating that the shift is due to changes in screening. A calculation of the change in $|\psi_s(0)|^2$ per p electron is made using the Fermi Segré formula and empirical screening coefficients due to Slater.

From the theory of electronegativity, a monotomic change of isomer shift from Li to Cs would be expected. The large departure from this prediction is unusual but not too surprising as the whole range of shifts in the alkali iodides is small and other effects can swamp that of electronegativity. In particular, it is suggested that the 5p electron distribution in CsF and RbI is distorted by dipole-dipole interaction; the polarizability of the alkali ion increases by a factor of 110 from Li to Cs. This interaction decreases the 5p population from LiI to CsI and hence $|\psi_s(0)|^2$ is larger in Rb and Cs iodides. This interpretation indicates that $\frac{\delta R}{R}$ is positive.

The iodates show positive shifts of 1.0 to 1.5 mm sec^{-1} and the periodate one of - 2.3 mm sec^{-1}. X-ray data show that in $(I O_3^-)$

compounds the I atom is surrounded by 6 oxygen atoms. The bond angles are close to 90° and the bonds will contain chiefly 5p electrons. Hence the shifts are positive. In the $(I\ O_4)^-$ ion, each I atom is surrounded by a tetrahedron of O with 109° between I-O bonds. This requires considerable sp hybridization, leading to removal of s electrons from I. A rough quantitative estimate gives .61 for the ionicity of the I-O bond in KIO_4. Electronegativity considerations suggest 0.4 - 0.5. The result, $\frac{\delta R}{R} = 3 \times 10^{-5}$, is difficult to explain using the single particle shell model; but if it is interpreted as due to a change in deformation, it can be related to the difference in quadrupole moments of the two states. Fair agreement is reached in the weak coupling (particle to core) approximation.

Interesting results have been obtained by Atzmony and Ofer (1965) on isomer shift ratios in Eu^{151} and Eu^{153}. One would expect that if it is justifiable to separate the isomer shift into the product of a nuclear part and an electronic part, the ratios of isomer shifts of a series of compounds should be the same for all nuclear transitions in the same element. Eu has three transitions which can be used, one in Eu^{151} and two in Eu^{153}. If the shifts measured in Eu_2O_3, Eu metal and Eu SO_4 are represented by a, b and c, then the quantity $\frac{a-b}{b-c}$ was found to take the values * for the

---

* 1.92 ± 0.14, 1.4 ± 0.25 and 1.24 ± 0.1.

three transitions. Atzmony and Ofer suggest that the discrepancies may be explained either in terms of polarization of the nucleus, since the nuclear deformation is known to be changing rapidly in the vicinity of Eu, or else as being due to the influence of $p_{\frac{1}{2}}$ electrons which are ignored in the usual treatments of the isomer shift.

It should be pointed out, however, that Kienle has also made a series of isomer shift measurements on Eu (reported at the 1965 Vienna Conference on the Mossbauer Effect) without observing any anomalies of the type reported by Atzmony and Ofer.

It might be expected that there should be an intrinsic dependence of isomer shift on temperature (at constant volume) due to the fact that the electrons follow the lattice vibrations almost adiabatically and hence their time-averaged density is related to the mean inverse volume of the unit cell, whereas the macroscopic density of the crystal depends on the mean volume of the cell.

This effect is, however, completely swamped by the second order Doppler shift (Josephson (1960); Pound and Rebka (1960) which accounts for about 90% of the temperature dependent shift in Fe. The remaining 10% can be ascribed, within experimental error, to thermal expansion. The volume dependence has been measured by Pound, Benedek and Drever (1961) who measured the shift as a function of pressure. Recently this work has been extended by Edge Ingalls Debrunner Drickamer and Frauenfelder (1965).

It is possible that in cases where the coefficient of

expansion is markedly anisotropic a further shift may arise due to a redistribution of electron wave functions with the change in bond angles.

The relativistic temperature shift referred to above can be derived either as a second order Doppler effect, or by the following argument due to Josephson.

When a nucleus emits a photon of energy E, its mass decreases by

$$\delta M = \frac{E}{c^2}$$

This causes a rise in the frequencies of all the normal modes of the crystal. The average fractional change of frequency will be $\delta M/2NM$ where NM is the total mass of the crystal.

If the photon is emitted without recoil, the occupation numbers of the various lattice modes do not change and therefore the energy of the crystal increases by $\delta E = \frac{E}{2NMc^2} U$ where U is the contribution to the internal energy arising from the lattice vibrations. Therefore the shift, in velocity units, between two temperatures T_1 and T_2 is

$$\delta v = \frac{1}{2c} \int_{T_1}^{T_2} C_v \, dT$$

where C_v is that part of the specific heat at constant volume which is associated with lattice vibrations.

This effect can sometimes usefully be employed to supplement measurements of recoiless fraction in lattice dynamical studies.

QUADRUPOLE SPLITTING

We will consider next the contribution to the energy of the system due to the interaction of the nuclear quadrupole moment, eQ, with the gradient of the electric field.

Q is defined as $\frac{1}{e}\int\rho(3z^2 - r^2)dxdydz$ where ρ is the charge density, e is the charge of the electron and the z axis coincides with the spin axis of the nucleus.

If the field gradient is referred to its principal axes it can be specified by $V_{zz}(= \partial^2V/\partial z^2)$ and $\eta\left(= \frac{V_{xx} - V_{yy}}{V_{zz}}\right)$ where $V_{zz} > V_{xx} \geqslant V_{yy}$ eq is often written for V_{zz}.

The Hamiltonian describing the interaction is

$$H_Q = \frac{e^2qQ}{4I(2I-1)}\left\{3I_z^2 - I(I+1) + \frac{\eta}{2}\left(I_x^2 - I_y^2\right)\right\}$$

A general expression for the eigenvalues cannot be given, but the secular equation has been solved for a number of special cases.

In the case of an axially symmetric field gradient ($\eta = 0$) the eigenvalues are:

$$E_Q = \frac{eqQ}{4I(2I-1)}\left\{3m_I^2 - I(I+1)\right\}$$

The relative intensities and angular distributions can be calculated by taking m_I to be a good quantum number.

Notice that the levels $\pm m_I$ are degenerate and also that the levels are not evenly spaced.

In the case $\eta \neq 0$, for $I = 3/2$, $E_Q = \pm\frac{e^2Qq}{4}\sqrt{1+\eta^2/3}$ (Q

vanishes for I = 1/2).

For all other cases of half integral spin also, the levels are degenerate, but for integral values of I, the degeneracy is removed.

$$\text{e.g. for } I = 1,\ E_Q = -\frac{e^2qQ}{2};\ \frac{e^2qQ}{4}(1 \pm \eta)$$

$$\text{for } I = 2,\ E_Q = \frac{1}{4}e^2qQ;\ \pm\frac{1}{4}e^2qQ\,(1 - \eta/3)^{\frac{1}{2}};\ -\frac{1}{8}e^2qQ(1 \pm \eta).$$

Unless η is sufficiently small for its effect to be treated as a small perturbation, these eigenvalues do not correspond to definite values of m_I and the intensities and angular distributions must be calculated by the methods described by Zory (1964). See also Bersohn (1952) or Das and Hahn (1958).

In order to analyse the quadrupole splitting, it is desirable that either the source or the absorber should have an unsplit single line spectrum, as otherwise the observed spectrum will have the form of a convolution of the two patterns and may be rather hard to interpret. If the number of lines in the spectrum is large and the recoilless fraction small, it is usually preferable to use an unsplit source and split absorber. The reason is that with this arrangement the whole of the incident radiation is at resonance with each of the absorption lines in turn, and it is only necessary to increase the absorber thickness to obtain the same maximum absorption as if both source and absorber were unsplit. With a split source and unsplit absorber only one of the lines in the incident spectrum is absorbed at a time and all the others contribute to the non-resonant back-

ground.

These considerations apply equally to magnetic splitting of course.

An unsplit line can be obtained by placing the resonant nucleus in a cubic environment. (Notice that it is not sufficient for the crystal as a hole to have cubic structure if the unit cell is at all complicated). This is not always easy and single line Mossbauer sources of rare earth elements for example are usually broadened by unresolved quadrupole splitting. (The other main source of broadening is an isomer shift which is not the same for all nuclei due to inhomogeneity in the surroundings). It has occasionally even been found necessary to go to the extreme of using a single member of a widely split absorption spectrum in place of a single line to analyse a source showing much smaller splitting.

The electric field gradient can be considered as being the sum of two contribution. The first is due to the asymmetry of the wave function of the electrons in the ion of which the nucleus forms a part, while the second is the resultant of the field gradients produced by the charges on each of the surrounding ions. The first of these terms can easily be calculated if the orbitals of the bonding electrons are known.

If the crystal has cubic symmetry, the field gradient will always average to zero, but if there is Stark splitting of the electronic levels by the crystal field, each sublevel will contribute a different field gradient. At temperature sufficiently

high for Stark levels above the lowest to be populated, one can usually expect that the relaxation time between them will be very short compared to the Larmor period of the nucleus, h/E_Q, and therefore one will observe an average of the field gradient taken over the Stark levels weighted with the Boltzman factor. Only when the temperature is so high that all the Stark levels are equally populated will the field gradient average to zero. (This, as will be seen later, is rather different from the behaviour of the magnetic interaction). Observation of the temperature dependence of the quadrupole splitting can thus be used to give information about the levels of the ion in the crystal field.

The field gradient calculated in this way must be corrected for the shielding of the nucleus by the closed electron shells which are themselves distorted by the field gradient. This correction is typically positive and of the order of 25%. Values have been calculated for a fair number of elements by Sternheimer and by others.

The second contribution is also in principle straight forward to calculate but often turns out to be very sensitive to small changes of lattice parameters, and in addition it is necessary to make an estimate of the charge to be associated with each ion.

The field gradient produced by external ions is also modified by the resultant distortion of the electron wave functions. This time the shielding factor turns out to be large and negative (i.e. the field gradient at the nucleus is increased). Typical values

of this "antishielding factor" lie around 100. Again, calculations have been made for a number of elements.

When shielding is taken into account, it turns out that these two contributions to the field gradient are often of the same order of magnitude. However, they are distinguished by the slight temperature-dependence of the second term.

It is quite possible for these two contributions to the field gradient to have opposite signs, in which case they may cancel at some temperature. However, the cancellation will usually not be complete unless the crystal has axial symmetry, since otherwise the components of the field gradients parallel and perpendicular to the z axis will generally vanish at different temperatures. This effect was demonstrated by Mossbauer and Poindexter (1964) who showed that the observed line width in $Tm_2^{169}O_3$ had a minimum value at a temperature of a few hundred degrees. This should be useful in the case of rare earths, which are seldom found in lattice sites having cubic symmetry and for which it is therefore difficult to obtain narrow single-line sources. Unfortunately it is seldom possible to work at the high temperature required, owing to the resulting low recoilless fraction.

In a magnetically ordered material, the exchange interaction will be large compared to the splitting in the crystal field and will therefore determine the magnitude of the electric field gradient. This situation will be considered later.

As was pointed out earlier, for nuclear spins greater than 3/2,

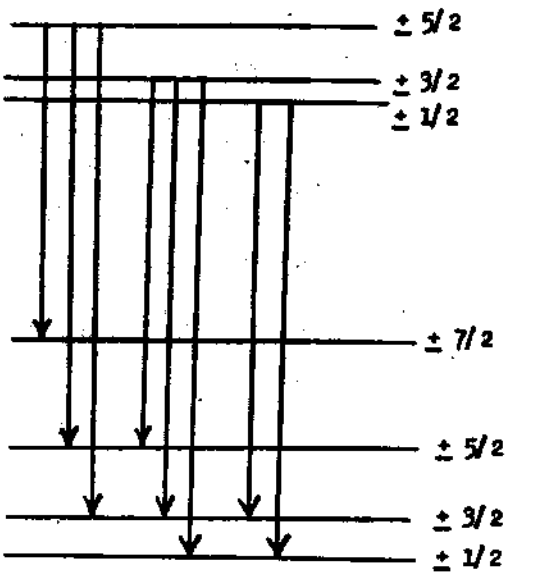

the levels are not uniformly spaced and it is therefore possible, from inspection of the Mossbauer spectrum, to decide the sign of eqQ for both levels. The figure illustrates this for the case of a nucleus having spins of 5/2 and 7/2 in the excited and ground state respectively. If the asymmetry parameter is equal to zero the levels may be assigned definite m-values and only those transitions allowed by the selection rule $\Delta m = 0$ or ± 1 (for dipole radiation) need be considered. This gives 8 transitions and it is easily seen that the relative positions of the lines will be changed completely if the order of the sub-levels of one of the states is reversed. The identification of the lines is further assisted by the fact that the intensities of the transitions are proportional to the Clebsch-Gordon coefficients (for a polycrystalline sample).

The example just considered is similar to the case of I^{129} which has been described in detail by Hafemeister, De Pasquali and De Waard (1964).

In the case of levels of spin 3/2 the spectrum will be symmetrical for a polycrystalline sample. However if a single crystal is used, we can make use of the different angular distributions of the $\Delta m = \pm 1$ and $\Delta m = 0$ radiation to decide which line is which and hence deduce the sign of the quadrupole interaction. It should

be noted however, that the recoilless fraction may not be isotropic and this can give rise to lines of unequal strength, even in the case of 3/2 to 1/2 transitions (such as Fe^{57} and Sn^{119}) in polycrystalline absorbers, for which the intensity ratio of the $\Delta m = 1$ transition to the $\Delta m = 0$ transition will be

$$\frac{\int f(\theta)(1+\cos^2\theta)\sin\theta\ d\theta}{\int f(\theta)(5/3-\cos^2\theta)\sin\theta\ d\theta}$$

This was first pointed out by Gol'danskii, Makarov and Khrapov (1963a) and has been observed in a number of cases.

The sign of the quadrupole interaction may also be determined for a polycrystalline absorber by observing the effect of an applied magnetic field Ruby and Flinn (1964). See also Collins (1965).

If the ground state quadrupole moment is known (e.g. from atomic beam measurements) the Mossbauer results allow us to determine the excited state moment and the field gradient. Otherwise we must choose some simple compound for which we think we can calculate the field gradient and use this to find the moments.

As in the case of isomer shift measurements, one can frequently derive useful information about the structure of a range of compounds from the ratios of the quadrupole couplings observed in them.

Probably the most careful study of the quadrupole interaction in Fe^{57} has been that of Ingalls (1964) who measured the temperature dependence of the splitting in a series of ferrous compounds.

According to Hund's rule, the ground state of the Fe^{++} ion ($3d^6$) should be a $^5D_4$ state. In a distorted octahedral environment

five of the electrons will combine to make no contribution to the field gradient. The gradient will therefore be due entirely to the sixth electron which will be distributed between the available orbitals with a relative probability given by the Boltzman factor. The field gradient due to an electron with quantum numbers n, l, m_l can be calculated from the formula, given by Townes and Shawlow (1955)

$$q_{nlm} = -\frac{2e\,l(l+1)}{(2l+3)(2l-1)}\left\{1 - \frac{3m^2}{l(l+1)}\right\}\left\langle \frac{1}{r^3} \right\rangle$$

where the factor $\left\langle \frac{1}{r^3} \right\rangle$ can either be found from the radial distribution given by a Hartree-Fock calculation or, in suitable cases, deduced from optical hyperfine structure data since the dipole field of the electron at the nucleus also depends on $\left\langle \frac{1}{r^2} \right\rangle$. Following this approach Ingalls after correcting for screening and for the contribution from surrounding ions, found for the quadrupole moment of the 3/2 state the value, $Q = (0.29 \pm 0.02) \times 10^{-24}$ cm^2.

In ionic trivalent Fe compounds the splitting is much smaller than in the divalent compounds. The Fe^{+++} ion is in the state $^6S_{5/2}$ and hence there is no contribution to the field gradient from the ion itself (as is confirmed by the small temperature-dependence of the splitting). In cases where the crystal structure is sufficiently well known, the lattice sum can be evaluated using the expressions

$$V_{zz} = \sum_i e_i \frac{3\cos^2\theta_i - 1}{r_i^3}$$

$$\eta = \frac{1}{V_{zz}} \sum e_i \frac{3\sin^2\theta_i \cos 2\varphi_i}{r_i^3}$$

and the result multiplied by the computed antishielding factor. The value deduced for $Q_{3/2}$ by this method is in good agreement with Ingalls' result.

In the case of Sn^{119} the position with regard to the absolute value of the excited state quadrupole moment is a good deal less satisfactory, but use has been made of the relative splittings to draw conclusions about the structures of a number of Sn compounds including organic compounds. (Aleksandrov et al. 1963). Also Gol'danskii et al. 1963b).

The quadrupole moment has been determined by measuring the splitting in Sn O and SnS and calculating the field gradient from the known crystal structure, using the formula of Townes and Shawlow already quoted and a value for $\left\langle \frac{1}{r^3} \right\rangle$ from optical hyperfine structure data. To this was added an estimate of the contribution from the surrounding ions. The result obtained was $Q_o = -11^{+10} \times$ $\times 10^{-26}$ cm^2. The large error arises from the fact that no accurate calculations of the screening coefficients were available, moreover the internal consistency of the result is poor. All the measurements were made at one temperature (80^oK) so it was assumed that the ion was in its ground state. It should certainly be possible to improve on the accuracy of the figure quoted.

The sign of the quadrupole moment was determined from Mossbauer spectrum of tetragonal SnO in which the intensities of the lines were unequal. An X-ray examination of the absorber which was in the form of a crystalline powder showed that it was partial-

ly oriented, with the axis of symmetry along the direction of the X-ray beam. This information identified the stronger peak as the one originating in the m = $\pm$ 3/2 level and this, together with the sign of the calculated field gradient determined the sign of the quadrupole moment.

The case of Iodine is interesting since there are five odd A isotopes formed by the successive addition of pairs of neutrons to I^{125}. I^{125} and I^{127} have ground state spin 5/2 and first excited state spin 7/2 and in the other three the order of the levels is reversed. The quadrupole moments of all the ground states are known and Mossbauer measurements now give the excited state moments of I^{127} and I^{129}. It is found that if all seven known quadrupole moments are plotted against neutron number, they fall on two straight lines, one for spin 7/2 and the other for 5/2. Attempts to explain this result have not been successful since all nuclear models tried so far suggest that $|Q_{7/2}|$ should be greater than $|Q_{5/2}|$, whereas the reverse is the case.

MAGNETIC SPLITTING OF MOSSBAUER SPECTRA

The interaction between the nuclear magnetic moment and a magnetic field, $\underline{H}$, is given by the Hamiltonian:

$$\mathcal{H}_m = - g\mu_n \underline{I}\,\underline{H}$$

where g is the gyromagnetic ratio of the nucleus whose spin is I and μ_n is the nuclear magneton.

The corresponding eigenvalues are:

$$E_m = - g \mu_n H m_I \quad \text{where} \quad -I \leq m_I \leq I \tag{28}$$

Thus, in the absence of a quadrupole interaction, a level of spin I will be split into (2I + 1) equally spaced sublevels.

Most observations have been made on nuclei in ions which are themselves paramagnetic, but one can also introduce a diamagnetic ion into a ferromagnetic lattice or make use of an externally applied field. The last method is seldom used since few Mossbauer lines are narrow enough to permit the resolution of the splitting produced by conveniently obtained external fields.

The field at the nucleus can be written

$$H = H_e + H_{int}$$

where H_e is due to the surrounding electron and is given by

$$H_e = g_e \beta \left\{ \left\langle \frac{1}{r^3} \right\rangle \langle \underline{L} \rangle + \left\langle \frac{3r(\underline{S}\cdot\underline{r})}{r^5} - \frac{\underline{S}}{r^3} \right\rangle + \frac{8\pi}{3} \left\langle \sum (S^{\uparrow} - S^{\downarrow}) \right\rangle \right\} \tag{29}$$

where g_e is the gyromagnetic ratio of the electron, β is the Bohr magneton, $S^{\uparrow}$ and $S^{\downarrow}$ represent s-electrons with spin up and spin down.

The first term represents the field due to orbital motion, the second term is the dipolar contribution of the electron spins, and the last term is the Fermi contact term which gives the effect of the spin density at the nucleus and hence vanishes for all except s-electrons. The last term is important since the closed s-sub-shells will be polarized by the unpaired electrons in other shells, and this effect greatly exceeds the direct contribution.

The magnitude of this effect is difficult to calculate. In a metal there will also be an important contribution to this term due to the conduction electrons.

The other component of the field, H_{int} is:

$$H_{int} = H_o + \frac{4}{3}\pi M - DM$$

where H_o is the macroscopic applied field, M is the polarization of the lattice and D is the demagnetizing factor which depends on the geometry of the sample. The numerical factor in the second term is strictly correct only for a cubic lattice.

In the absence of spin-orbit coupling, for an ion situated in a crystal field and with no applied magnetic field, m_L and m_s would be good quantum numbers. It is a consequence of time-reversal invariance that only degenerate states will contribute to the magnetization of the ion. In the 3d group of transition elements the spin-orbit coupling is weak compared to the interaction of L with the crystal field, and the ground state is non-degenerate. As a result, the orbital contribution to the field is quenched and the magnetization is almost entirely due to the electron spin. That this description is only approximately true is shown by the fact that the g-values for metallic iron does differ slightly from the value for the free electron. In ferrous compounds the orbital contribution is quite significant and it is known that g-values may be as high as 2.25. The ferric ion is in an S state and so there should be no orbital contribution anyway.

The behaviour of the 4f transition elements is quite different

since the crystal field splitting is smaller than the spin-orbit interaction and hence the good quantum number in this case is J and we have to average in eq. (29) over all the L and S values contributing to a state of given J. Tables for calculating the field are given by Elliot and Stevens (1953). Since J may be either integral or half-integral, the degeneracy of the ground state in the crystal field will depend on whether the number of electrons on the ion is odd or even. Ions with an even number of electrons will have a non-degenerate ground state and the magnetic moment will be completely quenched.

We expect that the magnetic fields produced by an ion in a degenerate ground state in the crystal field will be equal and opposite and as a result, provided the degeneracy is not removed by an applied field, the magnetization of the ion will vanish if it is averaged over a sufficiently long time. As we are interested in observing the hyperfine splitting of the nuclear levels, the time scale is given by the Larmor precession period, τ_L, of the nucleus. That is to say we will observe the full splitting if the spin-lattice and spin-spin relaxation times of the ion are long compared to $\hbar/E_m$ and no splitting for relaxation times much shorter than τ_L. The behaviour in intermediate cases can be rather complicated. Notice that while the magnetic field depends on m the electric field gradient depends on m^2 and therefore the relaxation of the ion between states of +m and -m does not cause the latter to average out.

Now suppose that a magnetic field is present. This will

remove the degeneracy and the population difference between the +m and -m states will be governed by the Boltzmann factor, leading to an effective field at the nucleus which may greatly exceed the applied field. In a ferro or antiferromagnet, the exchange interaction will lead to a splitting of the atomic levels which is large compared to the crystal field splitting. Provided the relaxation time is short, the field seen by the nucleus should be given by a thermal average over the states of the ion. It should therefore have the same temperature dependence as the bulk magnetization. This has been shown to be so in a number of cases including metallic iron and Ytrium-Iron Garnet. If the crystal-field splitting is very small compared to the magnetic interaction it can be ignored altogether and the ion treated as if it were completely free, apart from the interaction with the local magnetic field. This is expected to be the case for the rare earths and leads to a rather simple prediction for the temperature variation of the quadrupole interaction with the nucleus.

At a temperature T, the magnetization relative to that at saturation will be:

$$\frac{\sum_{J_z=-J}^{J} J_z \exp\left(\frac{-g\beta H J_z}{kT}\right)}{J \sum_{J_z=-J}^{J} \exp\left(-\frac{g\beta H J_z}{kT}\right)}$$

where H is the Weiss local field and is, of course, itself temperature dependent.

At the same time the electric field gradient will be proportional to:

$$\frac{\sum_{J_z=-J}^{J} \left\{3J_z^2 - J(J+1)\right\} \exp\left(\frac{-g\beta H J_z}{kT}\right)}{J(2J-1)\sum_{J_z=-J}^{J} \exp\left(-\frac{g\beta H J_z}{kT}\right)}$$

Thus there will be a definite relationship between the effective magnetic field and the electric field gradient at the nucleus. The latter falls off much more rapidly with increasing temperature. This result of the free-ion approximation has been verified in the case of Dy^{161} in both the metal (antiferromagnetic) and in Dy-Iron-Garnet and also for Tm^{169} in $TmFe_2$.

The Hamiltonian for the case where magnetic and electric fields are present together is just the sum of the separate expressions already quoted. (It must be remembered, however, that the principal axes of the two fields may not coincide).

It is not possible to write down expressions in closed form for the eigenvalues except in certain simple cases. (Abragam 1961).

In the case where the quadrupole interaction is small ($e^2qQ \ll \mu H$), the correction to the positions of the levels given by eq. (28) will be

$$\frac{e^2qQ}{8I(2I-1)}\left\{3m_I^2 - I(I+1)\right\}(3\cos^2\theta - 1 + \eta\sin^2\theta\cos 2\varphi) \ldots\ldots\ldots \quad (30)$$

where θ and φ are the polar angles of H with respect to the axes of the e.f.g.

If the absorber is not a single crystal and the direction of H is not fixed with respect to the crystal axes, the quadrupole interaction will result in a broadening of the lines. Thus in a polycrystalline ferromagnet in zero applied field the angles θ and φ will be constant (except perhaps in closure domains if the crystal symmetry is low). If a magnetic field is applied and gradually increased, the magnetization will at first become aligned along the easy directions nearest to the field; at still higher fields rotation of the domains will occur and the lines of the Mossbauer spectrum will become broadened.

For the case of $\eta = 0$, Abragam quotes the result of a second order perturbation calculation which can be used even when eq^2Q is not small. In other cases the secular equation must be solved. Numerical results are tabulated by Parker (1956 and by Matthias et al (1962).

If $\eta = 0$ and the symmetry axis coincides with H the results are particularly simple; m remains a good quantum number and the eigenvalues are just the sums of those obtained for the magnetic and electric interactions alone. (Notice that this result differs from eq. (30) only by a constant factor. The two situations cannot be distinguished simply from the relative spacing of the

lines).

Finally, if the e.f.g. is not axially symmetric but has its principal axes parallel to H, the secular equation can be solved without much difficulty. For the important case of I = 3/2, the four solutions are:

$$E_m = \pm \frac{g\mu H}{2} \pm \frac{e^2qQ}{4}\left\{\left(1 + \frac{4g\mu H}{e^2qQ}\right)^2 + \frac{\eta}{3}\right\}^{\frac{1}{2}}.$$

It will be seen from the form of the above expressions that they allow us to find from the observed splitting not only the magnitudes of the magnetic and electric interactions but also the sign of the electric quadrupole interaction.

In the case where m can be regarded as a good quantum number we can predict the allowed transitions using the selection rules $\Delta m = 0, \pm 1$ for dipole transitions or $\Delta m = 0, \pm 2$ for quadrupole transitions. We can also write down immediately the relative intensities, angular distributions and polarizations.

Other cases must be dealt with by working out the eigenfunctions, as discussed by Zory (loc cit). We will simply point out here that the number of allowed transitions may be increased (e.g. 8 instead of 6 for Fe^{57}).

Further complication can arise from the fact that some crystals may contain the Mossbauer nucleus at two or more non-equivalent sites for which the principal axes may not be parallel.

A fully resolved spectrum obtained by the use of a single-line source and analysed in this way will allow us to find the magnitude

of the magnetic interactions in the ground and excited states and their relative sign and also the magnitude and sign of the quadrupole interaction in both states. If the ground state magnetic moment is already known this allows us to find the excited state moment and the magnitude of the field at the nucleus. Even if the ground state moment is not known or is very small (e.g. in even-even isotopes it is zero), we can still find the excited state moment if there is another isotope of the same element in which the Mossbauer effect can be used to find the field. For example the magnetic moment of the first excited state of Dy^{160} can be found in terms of the ground state moment of Dy^{161} using the measured splitting in the metal which is ferromagnetic at low temperatures. So far as the Mossbauer spectrum is concerned, it makes no difference whether the magnetic ordering responsible for H_e is ferromagnetic or antiferromagnetic. In fact, the Mossbauer effect provides one of the few techniques, apart from neutron scattering, for the study of sublattice magnetization in antiferromagnetic and ferrimagnetic materials and is often the simplest method for finding the Neel temperature. As an example, antiferromagnetic Fe_2O_3 is known to undergo a rotation of 90^o in the direction of the spins at a temperature of 250^oK. Observation of the Mossbauer spectrum as a function of temperature in this region shows no detectable change in H_e, but an almost exact reversal of the quadrupole interaction, (as would be expected since the e.f.g. comes almost entirely from the surrounding ions and so does not rotate with the spins). (Forester 1964).

A direct measurement of magnetic splitting will not tell us

the sign of the magnetic interaction.

In order to find the direction of H_e relative to the direction of magnetization of the ion we must use some indirect method. The simplest in the case of the ferromagnet is to add an external field and see whether the splitting increases or decreases.

Several precautions must be observed. In the first place, the relative intensities of the lines from a fully magnetized sample will be different from those observed when the domains are oriented at random. It is therefore best to make a comparison between a field which is just great enough to magnetize the sample to saturation and a much larger field. This precaution will also avoid a second source of error which lies in the fact that magnetostriction will always cause an initial increase in the magnitude of H_e. (The importance of this effect has been enphasised by Grant, Kaplan, Keller and Shirley (1964) who studied the field at the nucleus of Au in dilute alloys with Fe, Co and Ni). Thirdly, it is important not to work too near to the Curie temperature since the domain magnetization will then be a function of applied field.

It is sometimes desirable to measure the hyperfine field in a paramagnetic solute in a non-ferromagnetic host. The above method cannot then be used since the splitting will simply be proportional to the applied field. In this case one can make use of the fact that the $\Delta m = \pm 1$ transitions, when observed along the direction of the field, are circularly polarized in opposite senses. (The intensity of the $\Delta m = 0$ transitions is zero in this direction).

If then the source and absorber are both magnetized along the direction of observation the $\Delta m = +1$ transitions in the source will excite $\Delta m = \pm 1$ transitions in the absorber according to whether the hyperfine fields are parallel or antiparallel and the converse will be true for $\Delta m = -1$ transitions. The form of the spectrum then gives the relative sign of the hyperfine field in source and absorber. Note however, that appreciable quadrupole splitting will greatly complicate the interpretation of the observed spectrum. The use of this method is discussed by Blum and Grodzins (1964).

When the relaxation time of the ion is very short the effective field approximation in which we consider the nucleus as situated in a steady field obtained by taking the thermal average over the states of the ion usually gives, as we have seen, a good description of the observed hyperfine splitting.

When the relaxation time is long it may become necessary to take account of additional terms in the spin Hamiltonian which cannot be represented as an interaction of the nuclear moment with an effective field. The number of lines in the spectrum may be increased and the levels may no longer be uniformly spaced. A rather detailed theoretical treatment of the problem has been given by Afanas'ev and Kagan (1964). Here we will consider simply a few examples.

Suppose that the levels of the ion in the crystal field form a series of Kramers doublets $\pm 1/2$, $\pm 3/2$, ... Then in the absence

of an applied field, if the relaxation time is long we should observe a superposition of spectra corresponding to the fields produced by spins of $\pm 1/2$, $\pm 3/2$, etc. This has been observed by Wertheim and Remeika (1964) who studied dilute Fe^{+++} ions in Al_2O_3. The Fe^{+++} ion is in a ^6S state which splits into states with $S_z = \pm 1/2$, $\pm 3/2$ and $\pm 5/2$ with very small separation so that at 78^oK they are equally populated. Lines corresponding to fields of 550 kG and 330 kG were observed, but the spectrum corresponding to the $\pm 1/2$ state is unsplit since the relaxation time between the states + 1/2 and - 1/2 is much shorter than between any other pair of states. Johnson, Cranshaw and Ridout (1964) carried out a similar experiment using a polycrystalline absorber but went down to a much lower temperature (1.3^oK). At this low temperature, unequal populations of the levels became apparent and it was found, as expected, that the $\pm 1/2$ level lies lowest. In addition, the relaxation time of the $\pm 1/2$ level was now long enough to give a resolved spectrum. However instead of the ground and excited nuclear states being split into 2 and 4 sublevels respectively, the ground state splits into a doublet and two singlets and the excited state into three doublets and two singlets. The reason is that the off-diagonal term in the part of the spin Hamiltonian representing the hyperfine interaction, which can be ignored in the $\pm 5/2$ and $\pm 3/2$ spin states, where the terms which they connect are well separated, have to be taken into account in the $\pm 1/2$ state in which they connect degenerate levels.

Johnson et al also varied the relaxation time through the spin-

spin interaction by varying the concentration of Fe^{+++} ions. They observed, as expected, a broadening of the lines together with a gradual transfer of intensity from the split spectrum to an unsplit central line.

In the rare earth salts the splitting of the J_z states is about 100 times larger and so at low temperature only a single Kramers doublet will be populated. If the order of the levels is inverted as, for example in Dy_2O_3 (Nowik 1965) where the ground state has $J_z = \pm 15/2$, the relaxation time will be very long since transitions between the degenerate levels would require quite a large change of angular momentum. In this case the splitting can be observed up to quite high temperatures (over 70°K).

Somewhat different is the case of $FeNH_4(SO_4)_2.12H_2O$ (Ferric ammonium alum), studied by Obenshain et al (1965). This shows no splitting in zero applied field, but at low temperatures can be magnetized almost to saturation in fields of about 20 kG. The relaxation time is believed to be not very much shorter than the Larmor period. It is found that when the field and temperature are varied, not only are the outer lines of the spectrum broadened much more than the inner ones as H/T is decreased, but the relative spacing does not remain constant. No complete theoretical analysis of this situation seems to have been made as yet.

Because of the large effect of core polarization, it is difficult to draw firm theoretical conclusions from the measured values of H_2. For example, Watson and Freeman (1961) calculated the

value of H_{eff} in Fe^{+++} to be = 630 kG. Although this is in good agreement with the measured values for ferric compounds, which fall within the quite small range of -515 to -625 kG, it is the result of the near cancellation of two much larger terms, since the s-electrons lying inside and outside the 3d shell contribute spin densities which are respectively parallel and antiparallel to the 3d spins. The uncertainty in the theoretical value is therefore large.

At the time when the field of -330 kG at the Fe nucleus in metallic Fe was first measured it caused some surprise since a positive value had been predicted. The situation is quite complicated, since in addition to the net negative contribution from the spins of the 3d electrons referred to above, there will be a small positive contribution due to the partial unquenching of the orbital angular momentum and also effects due to the polarization of the conduction electrons. This polarization can arise either as a result of exchange interaction with the 3d electrons or through covalent s-d mixing. These two effects give fields of opposite sign and it cannot be predicted which will be greater.

By observing the field induced at the nucleus of a diamagnetic ion in dilute solution in a ferromagnetic metal, one might hope to observe the effect of conduction electrons alone. Experiments of this kind have been carried out using Sn^{119} in Fe Co and Ni by Boyle, Bunbury and Edwards (1960), and using Au^{197} in the same host metals by Grant et al (1964).

The results are difficult to interpret quantitatively however, since the spin density is likely to be very non-uniform over the unit cell and large differences are observed. For example the values found for the field at a Sn nucleus in Co were -27 kG and -53 kG respectively for cubic and hexagonal Co.

Rather more direct information can be obtained from a systematic study of the hyperfine interaction in series of Fe alloys. For example for Fe^{57} in Fe Co, Fe Ni and Cu Ni alloys, if the magnetic splitting is plotted against the average moment of the alloy, the results fall on a single smooth curve with relatively little overall variation. In fact, the large hyperfine field remains on the Fe nucleus even when the alloy has a composition very close to that at which its magnetization disappears.

Fairly successful attemps have also been made to correlate the observed splitting with the number of Fe nearest neighbours in Fe alloys by observing the broadening of the spectrum and recently it has been possible to resolve the effects of different neighbours by using dilute alloys of impurities with Fe. The technique is well exemplified by solutions of Si in Fe which provide one of the simplest cases. This alloy has been discussed by Granshaw, Johnson and Ridout (1964) who used a single crystal to show the anisotropy of the hyperfine field. The component of the dipolar field of an atom at a neighbouring site $\underline{r}$ in the direction of magnetization $\underline{M}$ will be proportional to $(3\cos^2\theta - 1)$ where θ is the angle between $\underline{M}$ and $\underline{r}$ (and so will the electric field gradient). Hence, in a b.c.c.

crystal, the effect of nearest neighbours will vanish if the magnetization is along the (001) direction since then $\cos\theta = 1/\sqrt{3}$, but for magnetization along the (111) direction two of the nearest neighbours have $(3\cos^2\theta - 1) = 2$ and six have $(3\cos^2\theta - 1) = -2/3$. Similarly when the magnetization is in the (001) direction, six second neighbours will have no dipole or quadrupole effects, and six will contribute to the field. Therefore any broadening of the spectrum seen when the magnetization is in the (001) direction must be due to second neighbours, while the effects of nearest neighbours can be observed by magnetizing in the (111) direction. The observed shifts were quite small and could be recognized only by careful study of the shapes of the outermost lines in the spectrum.

There has been a good deal of interest in the study of the magnetic properties of the rare earth metals by the Mossbauer effect, since many of them are both ferro and antiferromagnetic at different temperatures and some of them have unusual forms of magnetic ordering in the antiferromagnetic state. The determination of the excited state moments is also of interest from the point of view of nuclear structure theory, since in this region of the periodic table the nuclei show large distortions and one expects that the unified model of Bohr and Mottelson, possibly with modification to allow for the effects of pairing correlations, will give a fairly good description of the properties of the nuclear levels. Nearly all the rare earths have at least one suitable Mossbauer transition, although the energy is often rather high,

necessitating the use of low temperatures.

The Mossbauer spectrum of Dy^{161} in Dy metal has been studied over the whole range of temperature from 4.2°K to the Neel point at 177°K. The metal is ferromagnetic at very low temperatures but changes to a spiral antiferromagnetic structure at about 85°K. In the antiferromagnetic state, all the spin in a particular plane perpendicular to the c-axis are aligned along some direction in that plane. The next plane is similar but the direction of magnetization differs from the first plane by a definite angle θ, the magnetization of the next is rotated by a further angle θ and so on. The angle θ has been measured by neutron scattering and shown to depend on temperature. If the free-ion approximation still holds in the antiferromagnetic region, there should be no discontinuity in the magnitude of the hyperfine interaction as a function of temperature and the shape of the curve in the antiferromagnetic region should be that of a Brillouin function. This is just what is found experimentally. However it is observed that above about 140°K, the individual lines of the spectrum start to become broadened and they soon cease to be clearly resolved. The broadening seems to be greatest for the outermost lines of the spectrum, suggesting that the effect is due either to fluctuations of the field at a rate slower than the Larmor frequency, or to local variations of the field such as might be expected if the Neel temperature were altered by local strains in the crystals. It seems rather difficult to explain effects as large as those observed by means of local variations of strain, but a recent

theoretical paper by Kagan and Afanas'ev (1965) has pointed out that slow fluctuations of the effective field are predicted at temperatures near the transition temperature if the sub-lattice magnetization is properly treated using the spin-wave formalism. An attempt is being made at present to see how closely the predictions of this paper agree with the experimental results.

It should be pointed out that it is often rather difficult to obtain a single-line source of a rare earth element. Most of the rare earths become magnetically ordered at low temperatures even when in the form of very dilute alloys with diamagnetic metals. This may be due to a tendency to form intermetallic compounds which crystallise out in grains of relatively large size (several molecules). The salts often have long relaxation times and, in addition, it is difficult to find a compound in which the rare earth ion is in a truly cubic environment. For all these reasons, observed line widths are always several times as great as the widths predicted from the excited state lifetime. A source which has been successfully used in connection with the 26 keV transition of Dy^{161} is produced by the irradiation of an alloy consisting of about 1% of Gd^{160} in natural Mg, but this recipe has proved less successful in some other cases. If the alloy is to be prepared before irradiation (which is safer and much more convenient) it is, of course, essential to make sure that no troublesome activities will be induced in any of the other isotopes of any of the elements present. Whenever an alloy is used either as source or absorber it is usually essential to anneal it careful

ly to ensure that all the resonant nuclei find themselves in similar environments, and the same precaution should be taken even with pure metals after neutron-irradiation.

* * *

REFERENCES

Abragan (1961) - The Principles of Nuclear Magnetism, Oxford University Press.

Afanas'ev and Kagan (1964) - JETP. 18 1139.

Aleksandrov et al. (1963) - Proc. Dubna Conference on the Mossbauer Effect 20-1.

Atsmony and Ofer (1965) - Phys. Lett. 14 284.

Baijal (1964) - Phys. Lett. 13 32.

Bernstein and Campbell (1963) - Phys. Rev. 132 1625.

Bernstein and Newton (1965) - In Press.

Bersohn (1952) - J. Chem. Phys. 20 1505.

Bersuker, Gel'danskii and Makarov (1965) - JETP. In Press.

Black et al (1964) - Proc. Phys. Soc. 83 925
" " " 83 937
" " " 83 941
" " " 84 169

Blum and Gredzins (1964) - Phys. Rev. 136 A 133

Bodmer (1961) - Nucl. Phys. 21 347

Bonchev et al. (1963) - Proc. Dubna Conference on the Mossbauer Effect.

Boyle, Bunbury and Edwards (1960) - Phys. Rev. Lett. 5 553.

Boyle, Bunbury and Edwards (1962) - Proc. Phys. Soc. 79 416.

Boyle, Bunbury, Edwards and Hall (1961) - Proc. Phys. Soc. 77 129.

Boyle and Hall (1962) - Rep. Prog. Phys. 25 441.

Bunbury, Elliott, Hall and Williams (1963) - Phys. Lett. 6 34.

Collins (1965) - Bull. Am. Phys. Soc. 10 174.

Cranshaw, Johnson and Ridout (1964) - Proc. Internat'l. Conf. on Magnetism at Nottingham.

Crawford and Shawlow (1949) - Phys. Rev. 76 1310.

Das and Hahn (1958) - Nuclear Quadrupole Resonance Spectroscopy (Solid State Physics Suppl. 1).

De Wames and Lehman (1964) - Phys. Rev. 135 170.

Disatnik, Fainstein and Lipkin (1965) - Phys. Rev. In Press.

Edge, Ingalls, Debrunner, Drickamer and Frauenfelder (1965) - Phys. Rev. 138A 729.

Elliott and Stevens (1953) - Proc. Roy. Soc. A218 553.

Feldman and Horton (1963) - Phys. Rev. 132 644.

Forester (1964) - ORNL Report No 3705.

Frauenfelder et al. (1961) - Nuovo Cimento 19 183.

Glauber (1955) - Phys. Rev. 98 1092.

Gol'danskii, Makarev and Khrapov (1963a) - Phys. Lett. 3 344.

Gol'danskii and Makarov (1965) - Phys. Lett. 14 111.

Gol'danskii (1964) - The Mossbauer Effect and its Applications to Chemistry. Consultants' Bureau Inc.

Gol'danskii et al (1963b) - Proc. Dubna Conference on the Mossbauer Effect. 17-1 and 23-1.

Goudsmit (1933) - Phys. Rev. 43 636.

Grant, Kaplan, Keller and Shirley (1964) - Phys. Rev. 133A 1062.

Hafemeister, De Pasquali and De Waard (1964) - Phys. Rev. 135B 1089.

Hasony and Hillman (1965) - Phys. Rev. In Press.

Heberle (1964) - Bull. Am. Phys. Soc. 9 634.

Heitler (1949) - The Quantum Theory of Radiation, Oxford University Press.

Hohenemser (1965) - Phys. Rev. In Press.

Ingalls (1964) - Phys. Rev. 133 787.

Johnson, Cranshaw and Ridout (1964) - Proc. Internat'l Conf. on Magnetism at Nottingham.

Josephson (1960) - Phys. Rev. Lett. 4 341.

Kagan and Afanas'ev (1965) - JETP 20 743.

Kankeleit (1961) - Z. Phys. 164 442.

Kopferman (1958) - Nuclear Moments, Academic Press,

Longworth and Packwood (1965) - Phys. Lett. 14 75.

Maradudin (1964) - Revs. Mod. Phys. 36 418.

Margulies and Ehrman (1961)- Nucl. Instr. 12 131.

Matthias et al (1962) - Phys. Rev. 125 261.

Mitrofanov, Illarionova and Shpinel (1963) - Proc. Dubna Conference on the Mossbauer Effect.

Morrison, Atac, De Brunner and Frauenfelder (1964) - Phys. Lett. 12 35.

Mossbauer and Poindexter (1964) - Revs. Mod. Phys. 36 362.
Nowik (1965) - Phys. Lett. 15 219.
Obenshain, Roberts, Coleman, Forester and Thomson (1965) - Phys. Lett. 14 365.
Parker (1956) - J. Chem. Phys. 24 1096.
Pound, Benedek and Drever (1961)- Phys. Rev. Lett. 7 405.
Pound and Rebka (1960) - Phys. Rev. Lett. 4 274.
Ruby and Hicks (1961) - Westinghouse Materials Laboratory Report No. P-6155-2.
Ruby and Flinn (1964) - Revs. Mod. Phys. 36 351.
Shirley (1964) - Revs. Mod. Phys. 36 333.
Shirley, Kaplan and Axel (1961) - Phys. Rev. 123 816.
Singwi and Robinson (1964) - Phys. Lett. 8 248.
Singwi and Sjolander (1960) - Phys. Rev. 120 2211.
Townes and Shawlow (1955) - Microwave Spectroscopy.
Van Hove (1954) - Phys. Rev. 95 249.
Vischer (1963) - Phys. Rev. 129 28.
Walker Wertheim and Jaccarino (1961) - Phys. Rev. Lett. 6 60.
Watson and Freeman (1961) - Phys. Rev. 123 2027.
Wertheim and Remeika (1964) - Phys. Lett. 10 14.
Zory (1964) - ONR Report NR 018-304 No 4.

* * *